



NTNU – Trondheim
Norwegian University of
Science and Technology

Interfacial Characterisation of Gas-Liquid Interfaces Related to Gas Flotation in Offshore Produced Water Treatment

Dynamic Adsorption of Heteroatoms

Anja Johnsen

Chemical Engineering

Submission date: June 2014

Supervisor: Gisle Øye, IKP

Co-supervisor: Mona Eftekhardadkhan, IKP

Norwegian University of Science and Technology
Department of Chemical Engineering

Preface

This thesis was given by the Department of Chemical Engineering at the Norwegian University of Science and Technology. This thesis is part of a research program sponsored by ConocoPhillips, ENI Norge, Schlumberger Division MI EPCON, Statoil and Total. The thesis is a requirement for the degree Master of Science and was conducted in the period 22.january to 18.june 2014.

I would like to thank my main supervisor Gisle Øye for all the advice and guidance throughout the process. I would also like to give a special thank to my co-supervisor Mona Eftekhardadkah for valuable feedback, motivation and support during these weeks. I wish you the best of luck on all your endeavours.

During these twenty-one weeks classmates, friends and family have been essential for me, and I would like to thank some of them. Elisabeth, thank you for being you and supporting me throughout this work, and Marius, thank you for teaching me tricks and shortcuts in Excel and Word. And so to the most important supporters, my family, you are everything to me and I could not have done this with out you.

I declare that this is an independent work according to the exam regulations of the Norwegian University of Science and Technology.

Trondheim, 17.june 2014.

Anja Johnsen

Abstract

Produced water is the largest waste stream produced in the recovery of oil and gas. The processing of produced water occurs in several stages including gas flotation. Gas flotation is separation by gravity and the effectiveness of gas flotation is dependant on the size of the gas bubble, the distribution of bubbles and the degree of dispersion. The concentration of oil and the chemical content of the produced water play a role, along with the pH, viscosity and the interfacial properties between the oil, gas and brine. Interfacial tension, wettability and spreading coefficient is interfacial properties that are important for the effectiveness of gas flotation.

The aim of this thesis is to see how dynamic adsorption of heteroatoms affects the interfacial tension and properties of solutions with different concentrations and at different pH values. The chemicals used in this thesis are Pyridine, Phenol and 3-cyclopentyl propionic acid. The interfacial tension measurements were done on a Maximum Bubble Pressure Tensiometer, which measures the interfacial tension at short time scales.

Throughout this thesis three chemicals with different properties, concentrations and various pH have been used. Each chemical shows different behaviour in both MQ-water and synthetic brine. Pyridine shows similar behaviour for all the six concentrations at pH 2 in both MQ-water and synthetic brine compared to the other pH values. For pH 7 and pH 10 the influence of concentration is more severe. The influence of pH at the higher pH values is almost non-existing for Pyridine in MQ-water. For Phenol in MQ-water an increase in concentration will lead to a decrease in surface tension. The influence of pH on Phenol indicates that at lower pH values Phenol is more soluble. For Phenol in synthetic brine the changes in pH has no effect on the surface tension. When comparing the result for Phenol in synthetic brine and MQ-water it is clear that the solubility of Phenol decreases in synthetic brine, leading to more severe decrease in surface tension in MQ-water than in synthetic brine. For 3-cyclopentyl propionic acid the influence of concentration on surface tension is clear. The decrease in surface tension before equilibrium values are reached is larger for this acid, due to the size of the molecule. The surface tension for this acid seems to be dependent on pH at low and at high concentrations.

Sammendrag

Produsert vann er den største avfallsstrømmen produsert i sammenheng med utvinning av olje og gass. Før dette vannet kan slippes ut i havet eller pumpes tilbake i reservoarene må det gjennom noen renseprosesser som blant annet inkluderer gassflotasjon. Denne prosessen er separasjon ved hjelp av gravitasjon og effektiviteten av denne prosessen er avhengig av noen faktorer. Størrelsen på gassboblene, fordelingen av boblene i flotasjonskammeret og grad av dispersjon er noen eksempler på slike faktorer. Konsentrasjonen av olje og andre kjemikalier i det produserte vannet spiller også en rolle i effektiviteten, sammen med pH, viskositet og grenseflateegenskaper mellom olje-, gass- og saltløsning. Grenseflatespenning, fukting og spredningskoeffisienten er også viktige parametere i gassflotasjon.

Hensikten med denne oppgaven er å se hvordan dynamisk adsorpsjon av heteroatomer påvirker grenseflatespenningen og grenseflateegenskapene til løsninger med forskjellig konsentrasjon og pH-verdier. Kjemikalier som ble brukt gjennom denne oppgaven var Pyridin, Fenol og 3-syklopentyl propionisk syre. Måling av grenseflatespenning ble gjort ved hjelp av et *Maximum Bubble Pressure Tensiometer*, som måler grenseflatespenningen ved korte tidsskalaer.

Gjennom denne avhandlingen har tre kjemikalier med ulike egenskaper, konsentrasjoner og pH blitt brukt. Hvert kjemikal viser ulik atferd i både MQ-vann og syntetisk saltløsning. Pyridin viser lignende oppførsel for alle de seks konsentrasjoner ved pH 2 i begge MQ-vann og syntetisk saltoppløsning sammenlignet med de andre pH-verdier. For pH 7 og pH 10 er innflytelsen av konsentrasjonen mer tydelig. Innflytelsen av endring i pH ved de høyere pH-verdier er nesten ikke-eksisterende for pyridin i MQ-vann. For Fenol i MQ-vann vil en økning i konsentrasjon føre til en reduksjon i overflatespenningen. Innvirkningen av pH på Fenol viser at ved lavere pH-verdier er Fenol mer oppløselig. For Fenol i syntetisk saltløsning har endringene i pH-verdien ingen innvirkning på overflatespenningen. Når man sammenligner resultatet for Fenol i syntetisk saltløsning og MQ-vann, er det klart at løseligheten av Fenol avtar i syntetisk saltløsning, noe som fører til mer tydelig reduksjon i overflatespenning i MQ-vann enn i syntetisk saltløsning. For 3-cyklopentyl-propionsyre er innflytelsen av konsentrasjonen

på overflatespenning er klar. Reduksjonen i overflatespenning før likevektsverdier oppnås er større for denne syre, på grunn av størrelsen på molekylet.

Overflatespenningen for denne syre synes å være avhengig av pH ved lave og ved høye konsentrasjoner.

List of Figures

Figure 1: The figure shows a scheme over the production of oil and gas [2].	1
Figure 2: The figure shows relative abundance of heteroatoms in crude oil [11].	3
Figure 3: The figure shows a typical produced water treatment process [14].	5
Figure 4: The figure shows the main steps in a gas flotation process [17].	6
Figure 5: The figure shows the hydrodynamics involved in the rise of oil/gas bubbles [18].	7
Figure 6: The figure shows the approach and attachment process in gas flotation [18].	10
Figure 7: a) shows a sketch of a dissolved gas flotation unit, while b) shows a sketch of an induced gas flotation unit [20].	11
Figure 8: The figure shows how the surface tension changes with concentration, and where the CMC can be found.	12
Figure 9: The figure shows two mechanisms of surfactant adsorption, (1) or (2) [29].	15
Figure 10: a) shows the origin of surface tension, while b) shows the origin of interfacial tension [37].	18
Figure 11: The figure shows a pyridine molecule.	21
Figure 12: The figure shows a phenol molecule.	22
Figure 13: The figure shows a 3-cyclopentyl propionic acid molecule.	22
Figure 14: The figure shows the difference in time window between methods used for measuring interfacial tension [29].	24
Figure 15: The figure shows the principle of the maximum bubble pressure tensiometer [42].	25
Figure 16: The figure shows the plot of surface tension versus concentration.	27
Figure 17.: The figure shows the plot of surface tension versus concentration.	28
Figure 18: The figure shows the measured interfacial tension for Pyridine at different concentrations.	29
Figure 19: The figure shows the measured interfacial tension for Phenol at different concentrations.	30
Figure 20: The figure shows the measured interfacial tension for 3-cyclopentyl propionic acid at different concentrations.	31
Figure 21: The figure shows the influence of pH on the interfacial tension of Pyridine.	32
Figure 22: The figure shows the influence of pH on the interfacial tension of Phenol.	33

Figure 23: The figure shows the influence of pH on the interfacial tension of 3-cyclopentyl propionic acid.....	34
Figure 24: The figure shows the influence of pH on the interfacial tension of Pyridine in synthetic brine.	35
Figure 25: The figure shows the influence of pH on the interfacial tension of Phenol.	35
Figure 26: The figure shows the difference in interfacial tension for the solvents MQ-water and synthetic brine.	36
Figure 27: The figure shows the influence of synthetic brine on three different concentrations of Pyridine at pH 7.....	37
Figure 28: The figure shows the influence of synthetic brine on three different concentrations of Phenol at pH 7.....	37
Figure 29: The figure describes the variation in surface tension for the three chemicals used in this thesis.	38
Figure 30: The figure shows the relationship between interfacial tension and surface age for Pyridine at pH 2 in MQ-water.....	39
Figure 31: The figure shows the relationship between interfacial tension and surface age for Pyridine at pH 2 in synthetic brine.	40
Figure 32: The figure shows the plot of surface tension versus $\ln(c)$ and the corresponding linear relationship.....	41
Figure 33: The figure shows the plot of surface tension versus $\ln(c)$ and the corresponding linear relationship.....	42
Figure 34: The figure shows the plot of surface tension versus $\ln(c)$ and the corresponding linear relationship.....	43
Figure 35: The figure shows the plot of surface tension versus $\ln(c)$ and the corresponding linear relationship.....	44
Figure 36: The figure shows the plot of surface tension versus $\ln(c)$ and the corresponding linear relationship.....	45
Figure 37: 1) Represent a clean interface before molecules adsorb, 2) shows the case were molecules have adsorbed as soon as the interface was formed.	46

Table of Contents

Preface	I
Abstract	III
Sammendrag	V
List of Figures	VII
Table of Contents	IX
1 Introduction	1
1.1 <i>Oil Production</i>	1
1.2 <i>Produced Water in Oil Production</i>	1
1.3 <i>Heteroatoms Present in Crude Oil and Produced Water</i>	3
2 Theoretical Background	5
2.1 <i>Processing of Produced Water</i>	5
2.2 <i>Gas Flotation</i>	6
2.2.1 <i>Flow Patterns and Probability for Flotation</i>	7
2.2.2 <i>Stokes Equation</i>	8
2.2.3 <i>Approach and Attachment Process between Gas Bubble and Droplet</i>	9
2.2.4 <i>Two Main Methods of Gas Flotation</i>	11
2.3 <i>Surfactants</i>	12
2.3.1 <i>Micelles and Critical Micelle Concentration</i>	12
2.3.2 <i>Solubility and Salting Out Effect</i>	14
2.4 <i>Adsorption</i>	15
2.4.1 <i>The Gibbs Adsorption Isotherm</i>	16
2.4.2 <i>A Modified Ward-Tordai Equation and the Diffusion coefficient</i>	16
2.5 <i>Surface Tension and Interfacial Tension</i>	18
2.5.1 <i>Dynamic Interfacial Tension</i>	19
3 Experimental; Materials and Methods	21
3.1 <i>Pyridine, Phenol and 3-cyclopentyl propionic acid</i>	21
3.1.1 <i>Pyridine</i>	21
3.1.2 <i>Phenol</i>	22
3.1.3 <i>3-cyclopentyl propionic acid</i>	22
3.2 <i>Preparation of Samples</i>	23
3.2.1 <i>Ultrapure Distilled Water</i>	23
3.2.2 <i>Synthetic Brine</i>	23
	IX

<i>3.3 Maximum Bubble Pressure Tensiometry</i>	24
4 Result and Discussion	27
<i>4.1 Determination of Micelle Formation for 3-Cyclopentyl Propionic Acid</i>	27
<i>4.2 Influence of Concentration</i>	28
<i>4.3 Influence of pH</i>	31
<i>4.4 Influence of Synthetic Brine</i>	36
<i>4.5 Pyridine at pH 2</i>	38
<i>4.6 Gibbs Adsorption Isotherm</i>	40
<i>4.7 Diffusion Coefficient; Diffusion Controlled or Mixed-Kinetic Diffusion Controlled</i>	45
5 Conclusion	47
6 Further Work	49
6 References	51
List of Appendices	55

1 Introduction

1.1 Oil Production

The production of crude oil is the most important source of energy, and accounts for around 40 % of the total energy consumption. Figure 1 shows a scheme of the production of oil from the exploration stage to the distribution to consumers. The crude oil resources are distributed unevenly around the world, with major supplies in the Middle East, and more limited resources in Europe and the United States [1].

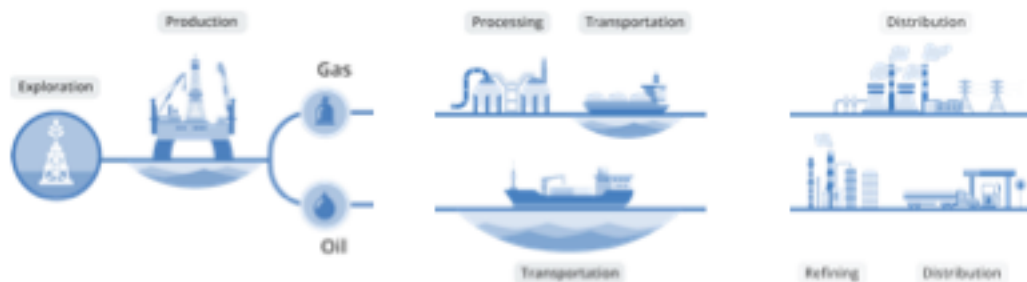


Figure 1: The figure shows a scheme over the production of oil and gas [2].

The major components in crude oil are hydrocarbons, and these hydrocarbons vary greatly in their molecular structure. The simplest hydrocarbons are chained molecules known as paraffins. Crude oil also contains a series of ring shaped hydrocarbons, known as naphthenes, which includes asphaltthenes. Aromatics are also ring shaped hydrocarbons were benzene is the main compound. Compounds containing heteroatoms (Sulphur, Nitrogen, Oxygen) and metals (Nickel, Vanadium) are non-hydrocarbon constituents in crude oil. The metal compounds occur in the more viscous crude oils [3].

1.2 Produced Water in Oil Production

Produced water is the largest waster stream produced in the recovery of oil and gas. Some of the water is present in the reservoir as a consequence of formation of hydrocarbons and some is there due to reinjection for oil recovery. The amount of

produced water present in a natural reservoir changes over time. In the initial life of the field the amount of produced water is low, but as the field ages more and more water is co-produced with oil and gas [4, 5]. These days the volume of water produced with production of oil and gas can make up as much as 90 % of all the fluids in one single well [6]. Produced water consists of water and a complex mixture of chemicals; the most common constituents are presented in table 1. The composition is highly dependent on the location of the reservoir, the hydrocarbons produced and of course the age of the field. The pH value of produced water normally lays around 6-7.7 [7, 8]. Most produced water has higher salt concentration than seawater, which leads to higher density.

Table 1: Show the most common constituents in produced water [7, 8].

Constituent	Description
Dissolved Solids	Inorganic constituents; Cl ⁻ , Na ⁺ , Ca ²⁺ , Mg ²⁺ , Fe ²⁺ , HCO ₃ ⁻ , CO ₃ ²⁻ , SO ₄ ⁻ .
Scales	Precipitated solids; CaCO ₃ , CaSO ₄ , FeSO ₂ .
Sand and suspended solids	Formation sand and clays, stimulation proppant and miscellaneous corrosion products.
Dissolved gases	Include natural gas; CH ₄ , C ₂ H ₆ , C ₃ H ₈ , C ₄ H ₁₀ . H ₂ S and CO ₂ .
Oil in Water Emulsions	
Dissolved Oil Concentrations	Hydrocarbons and other organic compounds with some solubility in water.
Dispersed Oil	Can consist of oil droplets in the size from 0.5 μm to 200 μm in diameter.
Production Chemicals	Chemicals from the drilling and production process.

The chemicals used in this thesis are dissolved oil concentrations in form of polar hydrocarbons and described in chapter 3.1 *Pyridine, Phenol and 3-cyclopentyl propionic acid*.

Produced water is apart of the “planned emissions” on the Norwegian Continental Shelf. These emissions are approved by the Norwegian government and controlled by laws and regulations. In Norway it is allowed to emit produced water containing a maximum of 30 ppm oil, though recent developments in technology used in produced water treatment allow emissions values below the official requirements [9, 10].

1.3 Heteroatoms Present in Crude Oil and Produced Water

Crude oil consists of small amounts of heteroatoms like sulphur, nitrogen and oxygen. The amount of sulphur present is low, but they cause difficulties when processing the crude oil. It is important to remove sulphur both from the crude oil and the produced water. Most of the nitrogen and oxygen species are present in resins and asphaltenes, which cause them to exhibit polar characteristics. The abundance of heteroatoms classes in crude oil is displayed in figure 2. The N_1 class species are the most abundant class of heteroatoms [11].

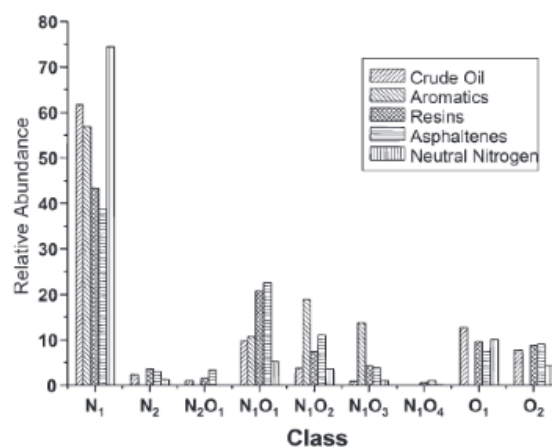


Figure 2: The figure shows relative abundance of heteroatoms in crude oil [11].

As seen in the figure the O_1 species are more abundant than the O_2 species.

The presence of heteroatoms in produced water is related to the water solubility of crude oil species. Hence, the abundance of species will change in comparison with the presence in crude oil. The most abundant species in produced water is O_x . The reason for this may be that the oxygenated functional group promotes aqueous solubility [12].

2 Theoretical Background

2.1 Processing of Produced Water

The processing of produced water occurs in several stages. As shown in Figure 3 the process usually starts with separation in 3-phase separators, before continuing to hydrocyclones and then the mixture enters a flotation unit and to remove the smallest particles the mixture is treated in filters [7, 8, 13].

The separation in the 3-phase separators takes place with the help of gravity. The gravity separation is done in two steps; the first step is done with high pressure and then followed by a second step with lower pressure. Oil is lighter than water and will therefore float to the top of the separators before continuing to a dehydrator and to oil export. The produced water left in the separators still contain impurities and is taken out for further processing [7].

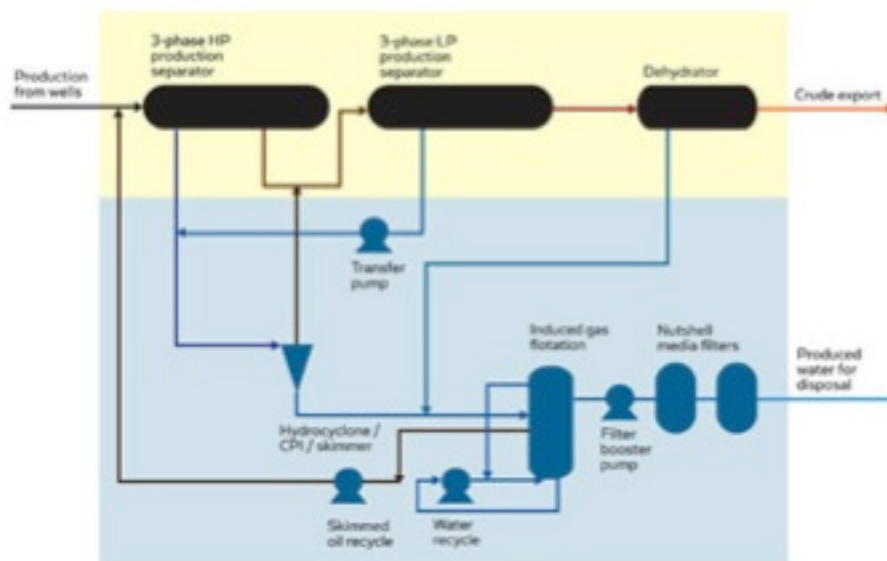


Figure 3: The figure shows a typical produced water treatment process [14].

The stage that follows is separation in hydrocyclones. Here centrifugal fields separate drops up to $15 \mu m$ and in ranges from 100 ppm to 2% oil in water emulsions. The efficiency of this kind of separation technique is up to 90% with ideal conditions. Separation with the help of hydrocyclones has some limitations, for example it cannot

remove particles at the oil/water interface, because such particles are a part of stable emulsions. These cyclones also have difficulties handling variations in flow [7].

The last stage in the water treatment process is executed with the use of filters. These filters are introduced for removal of dissolved organics. The shortcoming of these filters is that they require regenerating and they are expensive. Therefore, if the produced water is used for reinjection it does not need to be of high quality, so the filtration part of the treatment will than be unnecessary [15].

2.2 Gas Flotation

A flotation process consists of four basic steps, the generation of bubbles in the produced water, then the contact between a gas bubble and the oil droplet occur, before the attachment process take place and finally the combination of the gas bubble and the oil droplet will rise to the surface and be skimmed of. The three last steps are displayed in figure 4. The gas flotation process involves hydrodynamics and surface chemistry and is therefore considered a complex process [16, 17]. Gas flotation is an effective method for cleaning non-dissolved oil in produced water when the oil is heavy [18].

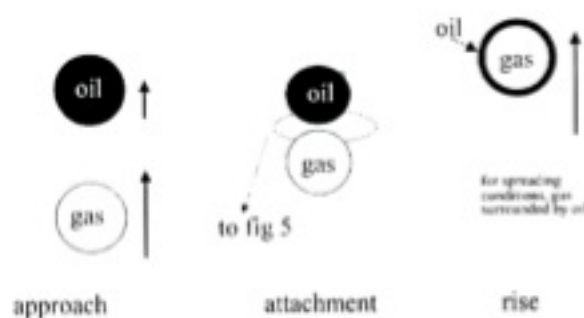


Figure 4: The figure shows the main steps in a gas flotation process [17].

The principle of gas flotation is that droplets or solids adhere to rising gas bubbles in a gas flotation chamber [18]. By attaching gas bubbles to the droplets, the effective density of the droplet is decreased, making the droplet appear lighter. This increases the density difference between the aggregate and water, causing the droplet to rise faster. So basically, the process is based on gravity separation [17].

The advantages of this process is that it can remove droplets down to $5\ \mu\text{m}$ and it can handle a large variation in the inlet fluid, which is an important factor when operating with produced water. One disadvantage of this process is that it may require additional gas. In offshore operations methane was commonly used, but due to explosion- and environmental hazards the use of this gas has been reduced. Inert gas, such as air may be used, but the increase in oxygen levels in the produced water may cause iron to precipitate. In flotation processes today, nitrogen is most common [17, 18].

2.2.1 Flow Patterns and Probability for Flotation

The bubbles can be generated in different ways, often by dissolution of a gas from a saturated solution, by mechanical mixing of gas and liquid or in some cases by gas injection[16]. Gas bubbles are introduced to the flotation chamber with the hope of collision. Figure 5 below shows a typical flow pattern of gas bubbles in a flotation chamber. As shown some of the droplets will move past the gas bubble and avoid collision and attachment [16].

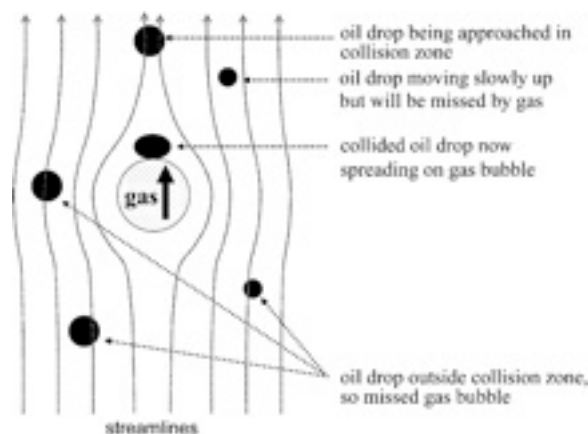


Figure 5: The figure shows the hydrodynamics involved in the rise of oil/gas bubbles [18].

Gas bubbles tend to be larger than oil droplets, and the difference in density between gas and water is greater than the difference between oil and water. According to this the gas bubbles rise faster than the oil droplets, which will lead to collision and attachment [16].

The probability for flotation can be calculated with the expression

$$P_f = P_c * P_a * P_s \quad (1)$$

where P_f is the probability for flotation, P_c is the probability of collision, P_a is the probability of adhesion and P_s is the probability of formation of a stable aggregate. The expression relates adhesion to the thinning and rupture of the films during the contact time and the formation of a stable aggregate is a function of the contact angle. The probability of collision between bubble and particle is directly related to bubble diameter, density, viscosity and the particle size. The rate-determining step in gas flotation is often looked at as the formation of a stable bubble-particle or bubble-drop aggregate. Such formations are made when the droplet attaches to the gas bubble [19].

2.2.2 Stokes Equation

Oil and gas are less dense than water and will, over time, rise to the surface if placed in water. An increase in the droplet size and the density difference as well as a decrease in the viscosity of the continuous phase will result in a rise rate which enables a residence time less than 30 minutes [18]. The smaller droplets give the slowest rise velocity. When the oil droplets attach themselves to the gas bubble the oil density is reduced, which then increases the density difference between the oil clusters and the water. The formations of clusters or agglomerates also increase the diameter, which leads to a faster rise rate. Stokes equation for the rise velocity for rigid spheres under laminar flow is shown in equation (2). It is known that gas bubbles are deformable, but the presence of surface active agents in the water will rigidify the interface, which causes the gas bubble to become a rigid sphere.

Stokes equation gives an understanding of the parameters affecting this rise velocity [17, 18].

$$V = \frac{d^2 g (\rho_w - \rho_o)}{18 \mu_w} \quad (2)$$

where V is the velocity, d is the droplet diameter, g is the gravitational acceleration, $(\rho_w - \rho_o)$ represents the density difference and μ_w is the dynamic viscosity. This equation states that the droplet diameter and the density difference are important parameters that will affect the rise velocity. One of the parameters is as mentioned droplet and bubble diameter, d . In order to get the diameter to a satisfactory level, the droplets need to coalesce [16-18].

The effectiveness of gas flotation is not only dependent on the different parameters in Stokes equation, but also on the size of the gas bubble, the distribution of bubbles and the degree of dispersion. The concentration of oil and the chemical content of the produced water play a role, along with the pH, viscosity and the interfacial properties between the oil, gas and brine. Interfacial tension, wettability and spreading coefficient is interfacial properties that are important for the effectiveness of gas flotation [18].

2.2.3 Approach and Attachment Process between Gas Bubble and Droplet

The approach between a gas bubble and a droplet is made possible by neutralizing the charge of the droplet. This is done by adding a chemical with an opposite charge. The charges of the droplet may cause repulsion, which will prevent coalescence and lead to a reduction in the attachment between droplet and gas bubble. To get droplets to coalesce chemical treatment with surface active agents is applied [16, 18].

The purpose of adding chemicals is to modify the charges at the interface. This will contribute to the coalescence of droplets and enable the attachment process. The chemicals used as surfactants may vary, if the agents are not suitable for the complex mixture in a particular produced water the spreading on the gas bubble will not occur and the gas bubble will reject from the droplet [18].

The attachment of an oil droplet on a gas bubble is displayed in figure 6, and if these do not occur within the time frame of approach the bubble and droplet will start to move further apart and as a consequence not attach [18].

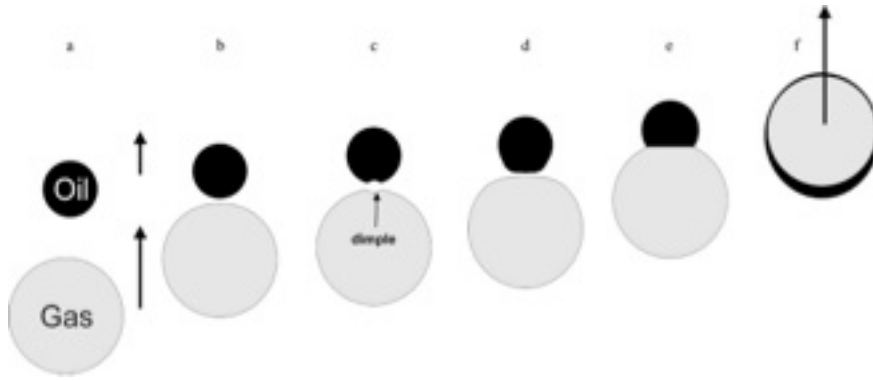


Figure 6: The figure shows the approach and attachment process in gas flotation [18].

The process starts when the gas bubble and oil droplet approaches each other. A thin layer or film of water is created when the gas bubble and oil droplet approaches each other, and as the bubble and droplet moves closer the liquid is squeezed out. This is commonly referred to as drainage of the film. When the film is drained a dimple is created at the surface of the droplet, this induces the pressure distribution over the film. The attachment process then continues with further thinning of the film until it eventually ruptures and spreads around the gas bubble. The boundary conditions at the interfaces are determined by the interfacial chemistry[16-18].

In the flotation process it is important to consider the low density of the droplets and the fact that they are not rigid bodies. As mentioned in subchapter 2.2.2 *Stokes Equation*, the droplets can be considered as rigid bodies when doing calculation, but in a flotation chamber the droplets will suffer deformation due to hydrodynamic forces. In addition to this the most characteristic effect is the spreading of the droplet on the gas bubble[16, 19].

After the bubble is attached it will start to spread on the surface of the bubble. The tendency of spreading is determined by the spreading coefficient, S_{ow} , which is defined by equation (3).

$$S_{ow} = \gamma_w - (\gamma_o - \gamma_{ow}) \quad (3)$$

where γ_w is the surface tension of pure water, γ_o is the surface tension of the oil and γ_{ow} is the interfacial tension between the oil and water [16, 18, 19].

In order to make a flotation process effective it is essential that the droplet and the bubble remain attached as they ascent in the flotation chamber [16].

2.2.4 Two Main Methods of Gas Flotation

In the industry there are two main methods of gas flotation, induced (dispersed) gas flotation (IGF) and dissolved gas flotation (DGF). The two methods are displayed in figure 7. In dissolved gas flotation the produced water is saturated with gas before entering the flotation chamber. The saturation happens under pressure and as the saturated water enters the flotation chamber the pressure is reduced, which releases gas bubbles. The bubbles are in the range of 20-100 μm and the retention time is around 15-30 minutes [19].

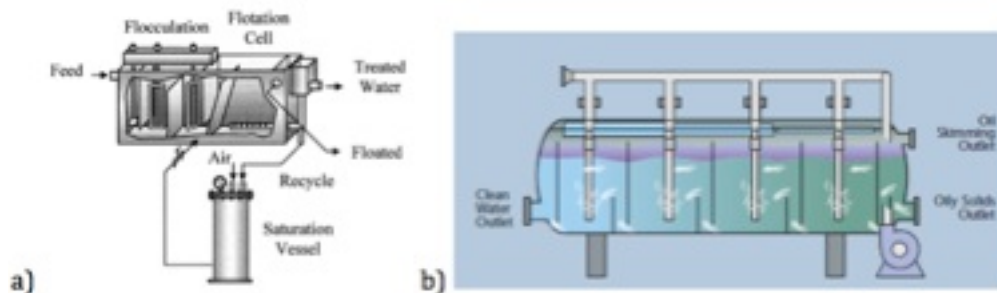


Figure 7: a) shows a sketch of a dissolved gas flotation unit, while b) shows a sketch of an induced gas flotation unit [20].

In induced gas flotation gas is past through a disperser before entering the flotation chamber, the gas bubbles are in the range of 1000 μm and the retention time in the chamber may be as low as four minutes [17].

The main differences between these two processes are the average bubble size and the mixing conditions.

2.3 Surfactants

Surfactants are surface active agents. They are characterized by their tendency to adsorb at surfaces and interfaces, and their amphiphilicity. Surfactants are amphiphilic, which means that they consist of two parts, a soluble (lyophilic) part and an insoluble (lyophobic) part. The polar head group is the soluble part while the attached hydrocarbon chain is the insoluble part. The composition of the polar head group and the hydrocarbon chain determines the amphiphilicity of the surfactant. The different surfactants are classified as anionic, cationic, non-ionic and zwitterionic, depending on the electrical charge of the molecule [21].

2.3.1 Micelles and Critical Micelle Concentration

One fundamental property of surfactants is the tendency to form micelles. Free surfactants, called monomers, in solution will at certain conditions form aggregates called micelles. This phenomenon is important, due to changes in behaviour when surfactants are present as monomers or in micelles. As seen in figure 8, the surface or interfacial tension will be lowered when free surfactant monomers are present in a solution, but not if surfactants are present as micelles. The concentration where micelles form is called the Critical Micelle Concentration, CMC [21].

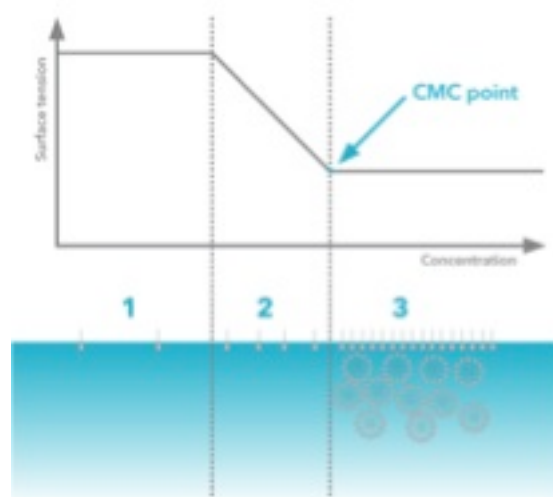


Figure 8: The figure shows how the surface tension changes with concentration, and where the CMC can be found.

The CMC affect the effectiveness of the surfactant by manipulating the droplet charge, which causes the droplets to repel each other instead of attracting each other. This decreases the efficiency of the flotation unit. The amount of added surfactant cannot exceed the CMC, if it does, micelles will start to form. The CMC varies with different conditions, some of them are listed below [22].

- The CMC decreases strongly with increasing alkyl chain length of the surfactant.
- Non-ionics have a lower CMC than ionics.
- Cationic surfactants have a higher CMC than anionics.
- The valency of the counterion is important. An increase in the valency of the counterion will give a decrease in CMC.
- Alkyl chain branching, double bonds, aromatic groups or some other polar character in the hydrophobic group will give a noticeable change in CMC.

In addition to these points, the effect of added electrolyte affects the CMC of ionic surfactants. The effect is larger for long-chained surfactants and more moderate for short-chained surfactants. Salt addition gives a lowering of CMC and a stronger variation in CMC with the number of carbons in the chain. The effect of added salt depends on the valence of the ions and it is most sensitive to the valence of added counterions. For non-ionic surfactants the addition of salt only gives small variations in the CMC, and both increase and decrease is possible [22].

2.3.2 Solubility and Salting Out Effect

Solubility is an important physical property that describes interactions between a solute and water [23, 24]. In general, large molecules are less soluble than small molecules, and principles such as “like dissolves like” should be remembered. The solubility of a molecule is also dependent on the shape of the molecule, because the shape determines the packing of the molecule, as well as the interactions with the solvent [23]. Aqueous solubility is related to hydrophobic surface area [25]. Polar functional groups, alkyl branching and aromatization decrease hydrophobic surface area, while alkyl chains increase hydrophobic surface area. In seawater electrostriction decreases the area, because hydrophobes may solvate between water molecules structured in cage-like formations [12, 26].

The salt concentration of produced water may vary from saturated brine to almost fresh water. The variations are dependent on the geology of the field and the processes used for production [27]. Solubility differs between water and sea water, because high molar volume or small or multivalent seawater ions “salt out” hydrophobic species [12]. The salting out effect occurs due to electrolytes present in water. The electrolytes strongly bind the water molecules together, which lead to the dehydration of the system [28].

2.4 Adsorption

Surfactants can adsorb and diffuse to an interface according to two different mechanisms, diffusion-controlled adsorption or mixed-kinetic diffusion. The two methods are displayed in figure 9 as (1) or (2), respectively [29].

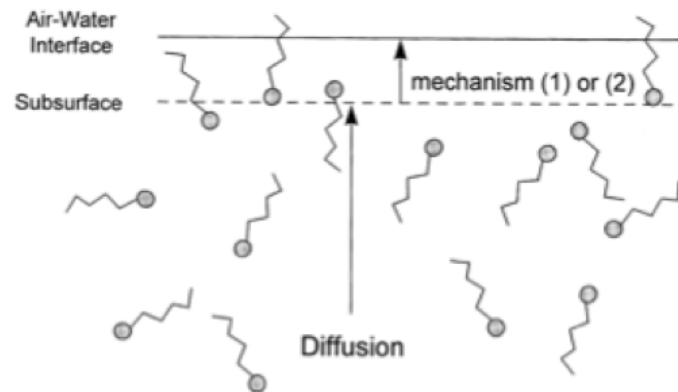


Figure 9: The figure shows two mechanisms of surfactant adsorption, (1) or (2) [29].

In diffusion-controlled adsorption the diffusion from the bulk to the subsurface is the rate-controlling step. The surfactant monomers diffuse from the bulk to the subsurface, and when the monomer reaches the subsurface the adsorption to the interface occurs immediately. The adsorption from the subsurface to the interface has a short timescale [29, 30].

Mixed-kinetic diffusion differs somewhat from the mechanism described above. In mixed-kinetic diffusion the rate-controlling step is the adsorption from the subsurface to the interface. The surfactant monomers diffuse from the bulk to the subsurface and when the adsorption to the interface is supposed to happen an adsorption barrier may occur, which will prevent the monomers to adsorb. This barrier can be related to the potential energy, reorientation of the surfactants or the access to vacant sites. These adsorption barriers may cause the molecule to diffuse back to the bulk instead of adsorbing to the interface, and as a consequence make the adsorption timescale larger than for diffusion-controlled adsorption [29].

2.4.1 The Gibbs Adsorption Isotherm

Gibbs adsorption isotherm describes the relationship between surface or interfacial tension, γ , and the surface excess, Γ (adsorption per unit area). For a surfactant solution at equilibrium, the interfacial concentration (surface excess) of a surfactant is given by Γ_{eq} . Gibbs equation is presented in equation (4), and enables the calculation of surface excess [29, 31, 32].

$$\Gamma_{eq} = -\frac{1}{nRT} \left(\frac{d\gamma}{d \ln c} \right) = -\frac{C_0}{nRT} \frac{d\gamma_{eq}}{dC_0} \quad (4)$$

where R is the gas constant, T is the temperature and $n = 1$ for non-ionic surfactants or ionic surfactant in the presence of excess electrolyte, and $n = 2$ for 1: 1 ionic surfactant, C_0 is the bulk concentration. The adsorption isotherm, Γ vs. C can be obtained by measuring the surface tension at different surfactant concentrations [31-33]. Surface tension, γ , and concentration, c , is measurable and the slope between γ and $\ln c$ gives Γ [29].

Equation (5) and (6) describe the relationship of the slope and the prefix of the surface excess.

$$\left(\frac{d\gamma}{d \ln c} \right) < 0 \Rightarrow \Gamma \text{ is positive} \quad (5)$$

$$\left(\frac{d\gamma}{d \ln c} \right) > 0 \Rightarrow \Gamma \text{ is negative} \quad (6)$$

The prefix of Γ describes if there is adsorption at the surface or depletion of solute from the surface, positive or negative, respectively.

2.4.2 A Modified Ward-Tordai Equation and the Diffusion coefficient

The Wang-Tordai equation is used to describe the adsorption kinetics at gas-liquid interfaces at curved surfaces. Liu, Wang and Messow modified the equation and solved it with Laplace transformation, which resulted in the three equations presented below.

Equation (7) represents the short-time limit adsorption with no back diffusion, equation (8) is for adsorption with back diffusion and equation (9) represents the long-time limit adsorption [30, 32, 34, 35]

$$\Gamma(t) = \sqrt{\frac{D}{\pi}} \left[2C_0\sqrt{t} - \int_0^t \frac{\phi(\tau)}{\sqrt{t-\tau}} d\tau \right] \quad (7)$$

where $\Gamma(t)$ is the dynamic surface adsorption, D is the diffusion coefficient, C_0 is the bulk concentration of surfactants, t is the time, $\phi(t)$ is the concentration of surfactants in the subsurface layer and τ is the integration variable [6, 32, 35].

$$\Gamma(t) = \frac{DC_0t}{r_0} + 2C_0\sqrt{\frac{Dt}{\pi}} \quad (8)$$

$$\Gamma(t) = (C_0 - C_s)\frac{D}{r_0} \left(t + 2r_0\sqrt{\frac{t}{D\pi}} \right) + Q \quad (t \geq t_1) \quad (9)$$

where r_0 is the radius of capillary, t_1 is a given long time where the concentration at the subsurface has reached a constant value, C_s , and Q is a function of t_1 and C_s [30, 34, 35]. By combining Gibbs equation, Eq. (4) and the equation for short time limit adsorption, Eq. (7), the dynamic surface adsorption can be expressed by the dynamic surface tension. This is done because $\Gamma(t)$ cannot be measured directly, while it is easy to obtain results when measuring the surface tension. The expression is presented in equation (10)[30, 32, 34].

$$\gamma(t) = \gamma_0 - \frac{RTD}{r_0} C_0 \left(\sqrt{t} + \frac{r_0}{\sqrt{\pi D}} \right)^2 + \frac{RT r_0}{\pi} C_0 \quad (10)$$

where $\gamma(t)$ is the dynamic surface tension and γ_0 is the equilibrium surface tension of the pure solvent. Equation (10) needs to be rearranged in order to calculate the diffusion coefficient. The rearranged expression is displayed in equation (11)[6, 32].

$$F = \sqrt{\frac{r_0(\gamma_0 - \gamma(t))}{RTc_0} + \frac{r_0^2}{\pi}} = \sqrt{Dt} + \frac{r_0}{\sqrt{\pi}} \quad (11)$$

Equation (11) states that there should be a linear relationship between F and \sqrt{t} . In some cases the bubbles created in the maximum bubble pressure tensiometer are so large that the surface can be characterized as planar [30]. For planar surfaces the equation used to calculate the diffusion coefficient changes to an easier form. The expression is presented equation (12)[34].

$$\gamma(t) = \gamma_0 - 2RTc \sqrt{\frac{Dt}{\pi}} \quad (12)$$

2.5 Surface Tension and Interfacial Tension

Surface tension and interfacial tension is related to the attractive forces between molecules in a liquid. These forces try to reduce the interfacial and surface area. As seen in figure 10 the surface tension originates as a consequence of asymmetry in the attractive forces, while for interfacial tension the imbalance in the attractive forces at the interface of the molecules is the origin for the interfacial tension [36].



Figure 10: a) shows the origin of surface tension, while b) shows the origin of interfacial tension [36].

The surface or interfacial tension of a solution containing electrolytes is higher than for pure water when it comes into contact with water. It is a known phenomenon that the rise in surface tension were considered to be caused by the repulsive interactions

between the ions and air, as a consequence the electrolyte ions are repelled from the air-water interface [37].

2.5.1 Dynamic Interfacial Tension

When a new interface is formed, the surface tension, γ , is the same as the tension for the bulk solution, γ_0 , but over time it will change and eventually reach an equilibrium value, γ_{eq} . The change in surface tension before equilibrium conditions are established is called dynamic surface tension, $\gamma(t)$. The change in surface tension can vary from milliseconds to days, and is dependent on the type of surfactant and concentration [29]. For larger molecules the migration to the interface and the orientation at the interface takes time, and as a consequence it takes time for changes in tension to occur, as well as to reach equilibrium. The most surface active components will compete for a place at the surface, and the compound that is most interfacial active will adsorb at the interface. At equilibrium the component with the lower interfacial tension will be in excess at the interface and cause a lowering in the interfacial tension between the components. [36, 38]. In this thesis the dynamic interfacial tension is measured, because the changes in interfacial tension occur before equilibrium values are reached.

3 Experimental; Materials and Methods

3.1 Pyridine, Phenol and 3-cyclopentyl propionic acid

Pyridine, phenol and 3-cyclopentyl propionic acid are the chemicals used throughout this thesis. These chemicals are polar hydrocarbons present in produced water as water-soluble hydrocarbons containing heteroatoms, such as nitrogen, oxygen and sulphur. Polar dissolved hydrocarbons can be classified based on the type and number of heteroatoms present in the molecule [20].

- Nitrogen-containing compounds.
- Oxygen-containing compounds.
- Sulphur-containing compounds.

3.1.1 Pyridine

Pyridine is an alkaline nitrogen-containing hydrocarbon with high water solubility. The main factor for the high water solubility is specific interactions between the hydrogen bonds. Pyridine exhibit weak base properties. As displayed in figure 11, pyridinic molecules contain a lone pair of electrons on the nitrogen atom, which will interact with the hydrogen atoms in water, making the molecule highly soluble [39]. Pyridine is a basic nitrogen-containing compound and they are highly abundant as positive ions in crude oil [12].

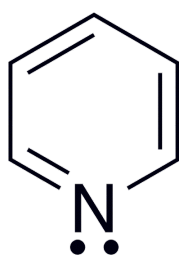


Figure 11: The figure shows a pyridine molecule.

3.1.2 Phenol

Phenol is an oxygen-containing and extremely water soluble compound, the water solubility will decrease with increasing molecular weight (alkyl chain length). Of all organic compounds found in produced water, the oxygen-containing compounds are present with the highest concentration. The O_1 -species are the second most abundant of the oxygen-containing species [12]. Figure 12 displays a phenol molecule. The most abundant phenolic species on the Norwegian Continental Shelf are phenol, methylphenol and the dimethylphenol [27].

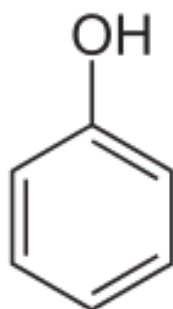


Figure 12: The figure shows a phenol molecule.

3.1.3 3-cyclopentyl propionic acid

3-cyclopentyl propionic acid is an O_2 -species. The molecular structure is presented in figure 13. This species is the most abundant species of the oxygen-containing compounds in produced water and contains fatty and naphthenic acids. The solubility of these compounds is affected by the presence of salt and the structure of the will determine the extent of the salting out effect.

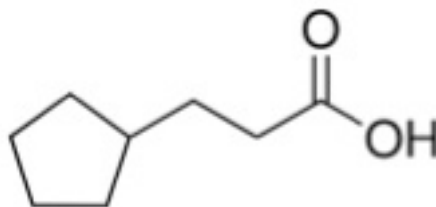


Figure 13: The figure shows a 3-cyclopentyl propionic acid molecule.

3.2 Preparation of Samples

In this thesis the chemical used were Pyridine, Phenol and 3-cyclopentyl propionic acid. Pyridine and phenol was mixed in two different water phases; Ultrapure distilled water and synthetic brine.

During this thesis 164 samples were made and analysed.

3.2.1 Ultrapure Distilled Water

The chemicals were first tested in ultrapure distilled water, also known as Milli-Q water. This was done to see how the different chemicals affected the interfacial tension of pure water.

3.2.2 Synthetic Brine

Produced water can be prepared in the laboratory by mixing crude oil and synthetic brine. In this thesis synthetic brine was used, which consisted of different salt. The composition of the brine is presented in table 2.

Table 2: The table shows the composition of synthetic brine.

Compound	Weighed in for one litre brine, [g]
NaCl	89,67
CaCl ₂ * 2H ₂ O	11,958
MgCl ₂ * 6H ₂ O	7,605
NaHCO ₃	0,3004
Na ₂ SO ₄	0,0665
H ₂ O	890,4

The preparation of the brine was done in an Schott bottle (1000ml). The different salts were dissolved, one by one, using Milli-Q water. The bicarbonate was dissolved last, in order to prevent precipitation. During the preparation of the brine the mixture was continuously stirred using a magnetic stirrer. The chemicals were added to see how they affect the interfacial tension of the brine.

The concentrations of the solutions measured were 100 mM, 70 mM, 50 mM, 30 mM, 10 mM and 1 mM. Each of the water phases was mixed with each chemical to make a bulk solution with the concentration of 100 mM, and subsequently diluted to obtain the other concentration. For each of the concentration there were made two parallels. The bulk solution was made in 250 ml Schott bottles and the other concentrations were prepared in 50 ml Schott bottles. For each of the parallels the pH was measured and adjusted to pH 2, 7 or 10. This was done using a SevenEasy™ pH meter. The adjustments are done by adding drops of 1 M HCl or NaOH. After the pH measurements were completed, the density measurements followed. These measurements was done for each concentration using a DMA-5000 Density Meter, Printer, Sample Handling Unit. The densities of the samples are essential when using the maximum bubble pressure tensiometer. For mass calculations, detailed values of pH and density see Appendix A.

3.3 Maximum Bubble Pressure Tensiometry

The dynamic interfacial tension can be measured by different methods. Some of these methods are displayed in figure 14. As shown in the figure, the methods differ in the time intervals down to milliseconds[29, 40].

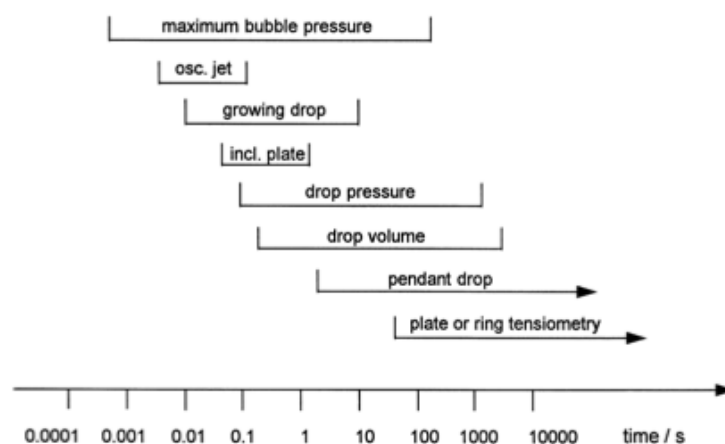


Figure 14: The figure shows the difference in time window between methods used for measuring interfacial tension [29].

In this thesis the measurement of the dynamic interfacial tension was executed on a maximum bubble pressure tensionmeter (Kruss, BP100). By using BP100 the surface age can be found from 5 milliseconds to 200 milliseconds. In this tensiometer gas bubbles are generated in a liquid sample using a capillary connected to a pressure sensor. The capillary radius is known and the bubbles enter the water phase through this capillary. The pressure must work against the surface tension of the sample to increase the bubble size. Dynamic interfacial tension can be measured as a function of the aging of the gas bubbles or as the surface age of the gas bubble. The surface age is the time from the beginning of the bubble formation and to the time the maximum pressure is detected. This is presented in figure 15[40, 41].

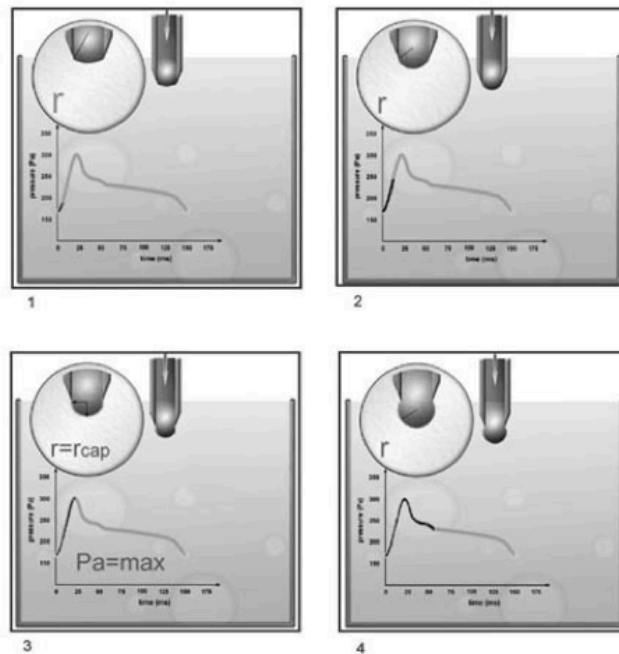


Figure 15: The figure shows the principle of the maximum bubble pressure tensiometer [41].

Picture one in the figure above shows when the bubble is formed. At this point the pressure is below the maximum pressure, the radius of curvature of the gas bubble is larger than the radius of the capillary. Presented in the second picture the pressure curve approaches the maximum, at this point the radius of the capillary is the same as the radius of the gas bubble. In the following picture the pressure reaches and passes a maximum. In equation (10) the relationship between the maximum pressure, P_{max} , the hydrostatic pressure in the capillary, P_0 , the inner radius r of the capillary and the surface tension, γ , is presented[34, 41].

$$\gamma = \frac{(P_{max} * P_0) * r}{2} \quad (10)$$

In picture four the pressure decreases again, the radius of the gas bubble becomes larger and the “dead time” of the measurement starts. Finally, the bubble escapes from the capillary and rises[41].

Before the measurements can be executed the capillary diameter must be determined. Sanding the capillary before measuring the diameter using the tensiometer does this. The surface tension of Milli-Q water is measured to ensure that the capillary has the proper hydrophobic coating, if the values lay around 72 mN/m the instrument is ready to measure samples. Such water tests are important to perform often, in order to ensure that the capillary is working properly. If the capillary is measuring wrong values the washing and sanding must be repeated or the capillary may need changing.

Between every measurement the capillary and sample vessel must be properly cleaned. The cleaning is done with hot water, than isopropanol (2-propanol) and thoroughly with Milli-Q water.

To start the measurement the clean capillary is tightened in the capillary holder, while 20-30 ml of a sample is poured into the sample vessel and placed on the sample platform. The platform is than raised until it is around one cm from the capillary tip. If the results deviate from theory or each other a sanding and a wash may be necessary.

For each sample measured 81 or 88 measurements were obtained. The number of measurements was depended on the selected measuring time, 100 milliseconds and 200 milliseconds, respectively. The measuring time varies from around 45 minutes to over one hour.

4 Result and Discussion

The chemicals used throughout this thesis were chosen based on their water solubility and the fact that they are present in produced water. Dibenzothiophene was intended to have a role in these experiments and was reported to show water solubility [12].

However, when mixed with water Dibenzothiophene showed no water solubility. As a result the chemical was excluded from further experiments.

Pyridine and Phenol displayed high water solubility, both in MQ-water and in synthetic brine. The acid, 3-cyclopentyl propionic acid, displayed high water solubility at high pH values in MQ-water, but at pH 2 the acid was only soluble at the lowest concentration, 1 mM. The surface tension measurements for the acid in synthetic brine were not conducted. When the chemicals are solved in synthetic brine the pH is adjusted to pH 2 and pH 7, due to precipitation at pH 10.

4.1 Determination of Micelle Formation for 3-Cyclopentyl Propionic Acid

When starting the experiments it was indicated that the acid, 3-cyclopentyl propionic acid, might form micelles in solution. To determine if micelles were present in the solution the surface tension was plotted against concentration, as displayed in figure 16 and figure 17 for pH 7 and pH 10, respectively. The values were obtained by taking the average of equilibrium values of the surface tension and the concentration is the six concentration used throughout this thesis.

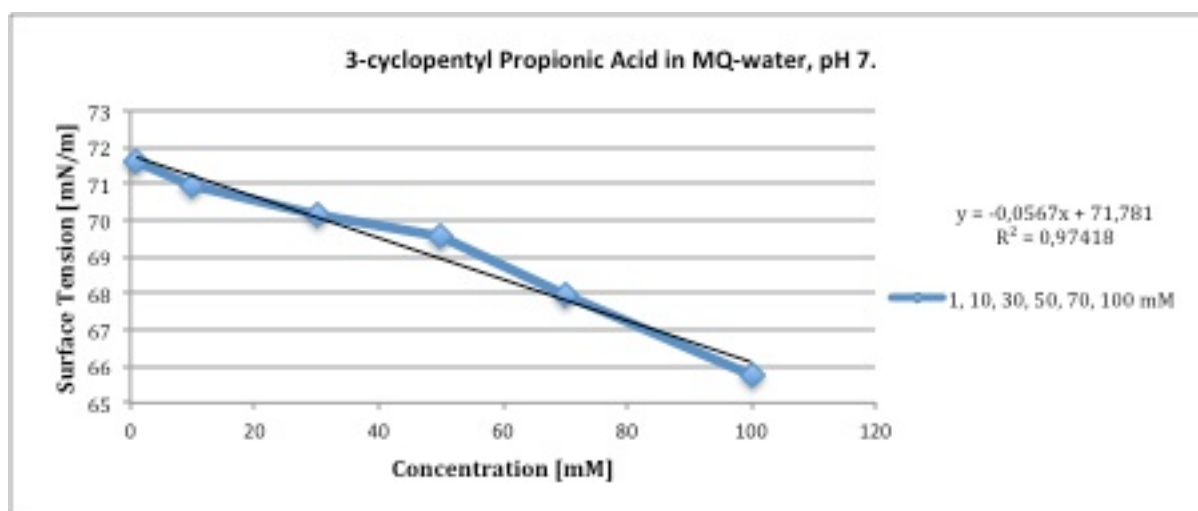


Figure 16: The figure shows the plot of surface tension versus concentration.

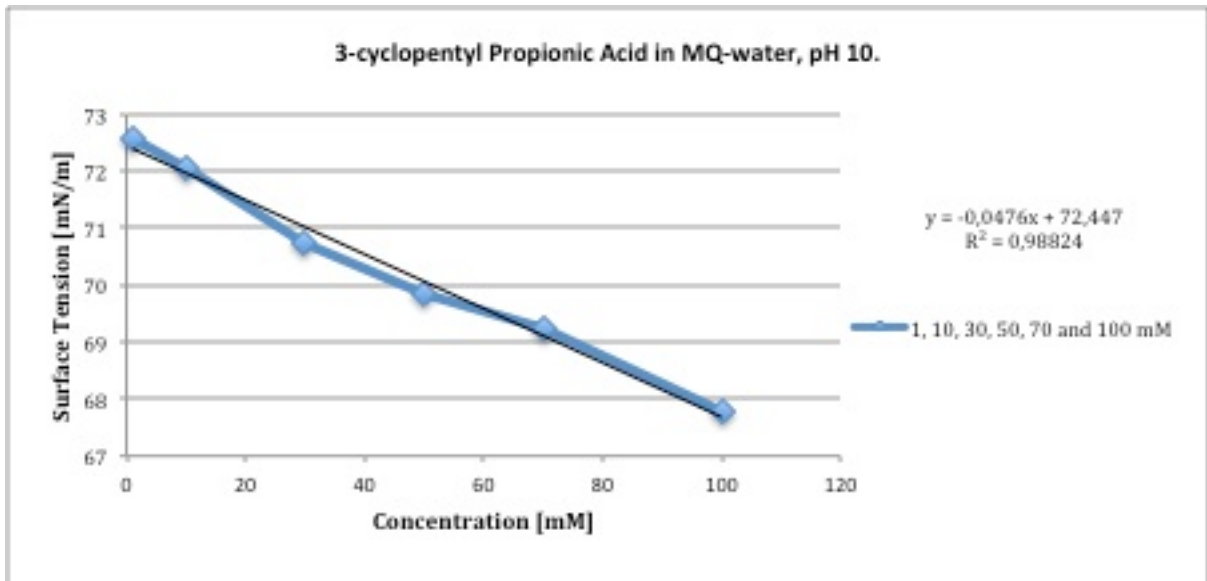


Figure 17.: The figure shows the plot of surface tension versus concentration.

In the theory on micelle a graph that indicates micelle formation is introduced. In comparison with the graphs above a difference is clearly observed, the deviation from linearity in the graphs above is minute, which indicates that no micelles are formed for the range of concentration used in this thesis.

4.2 Influence of Concentration

The lowering of interfacial tension is affected by the concentration of chemicals in solution. In MQ-water an increase in concentration of the solute will lead to a decrease in interfacial tension for the solution. In this section three figures are presented as examples, but the trends are common for all the plots. The remaining plots are listed in Appendix C.

In figure 18 the measured surface tension of Pyridine is plotted against the surface age at pH 7. In the graph it is clearly shown that the lowering of interfacial tension is dependant on concentration. The figure also display that the decrease in interfacial tension happen within the first 100 milliseconds and that equilibrium values are reached quickly. This indicates that the adsorption at the interface occurs directly after the bubble surface starts to form and that the diffusion is the rate-controlling step, making the adsorption diffusion controlled.

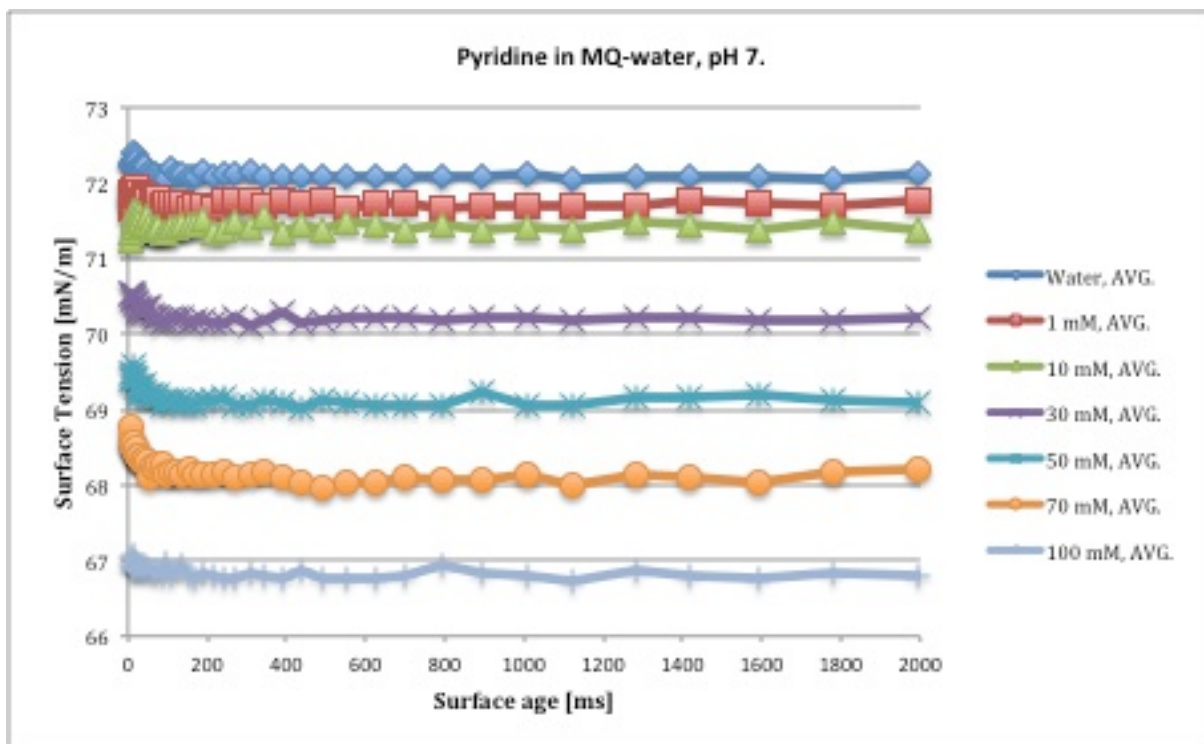


Figure 18: The figure shows the measured interfacial tension for Pyridine at different concentrations.

The plot of surface tension versus surface age for Phenol at pH 7 is presented in figure 19. The figure displays the same trends as for Pyridine. The main difference is that Phenol affects the lowering of interfacial tension more. As seen in the figure, the largest concentrations of Phenol lower the interfacial tension by around 5 mN/m more than the same concentration for Pyridine. This is because Phenol is more surface active.

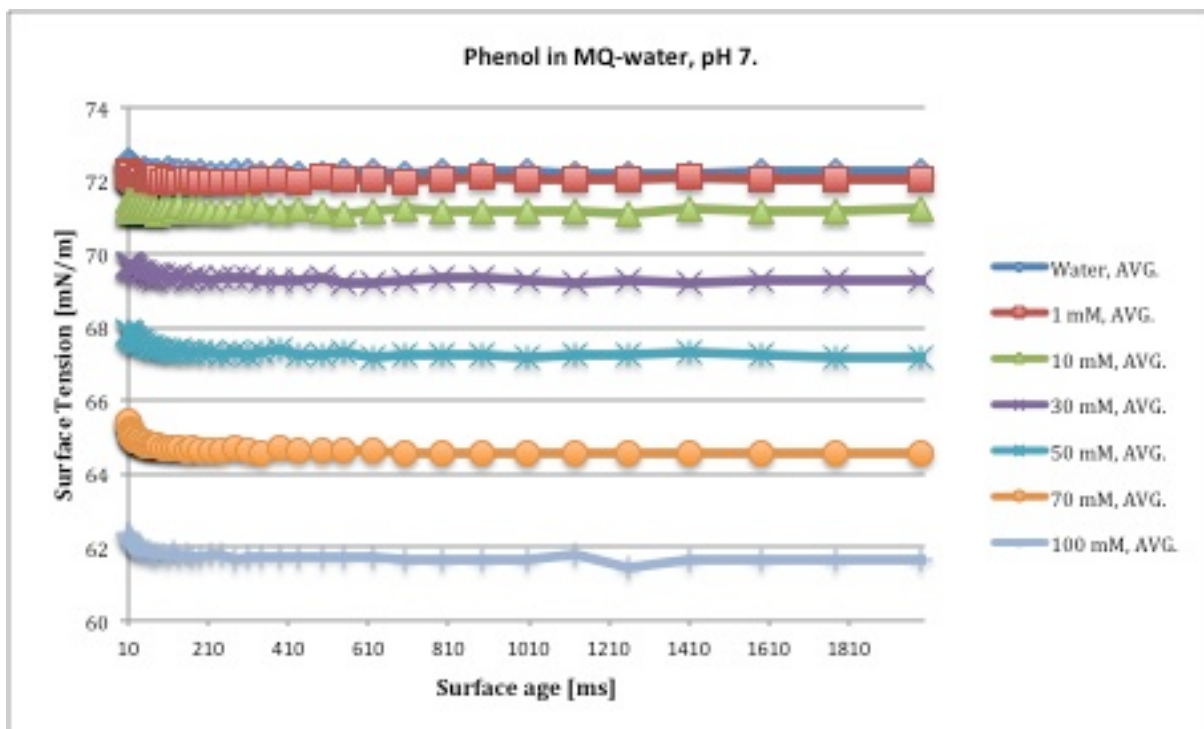


Figure 19: The figure shows the measured interfacial tension for Phenol at different concentrations.

Figure 20 describes the relationship between surface tension and surface age for 3-cyclopentyl propionic acid at pH 7. These plots differ slightly from the other chemicals, but the overall trend is similar. The main difference is that the time scale is slightly increased and the lowering of surface tension is more severe and occurs over several milliseconds. The lowering in surface tension before equilibrium values are reached is more severe for this acid than for the other chemicals. The acid has the slowest adsorption, meaning that the equilibrium is obtained in a larger range of time.

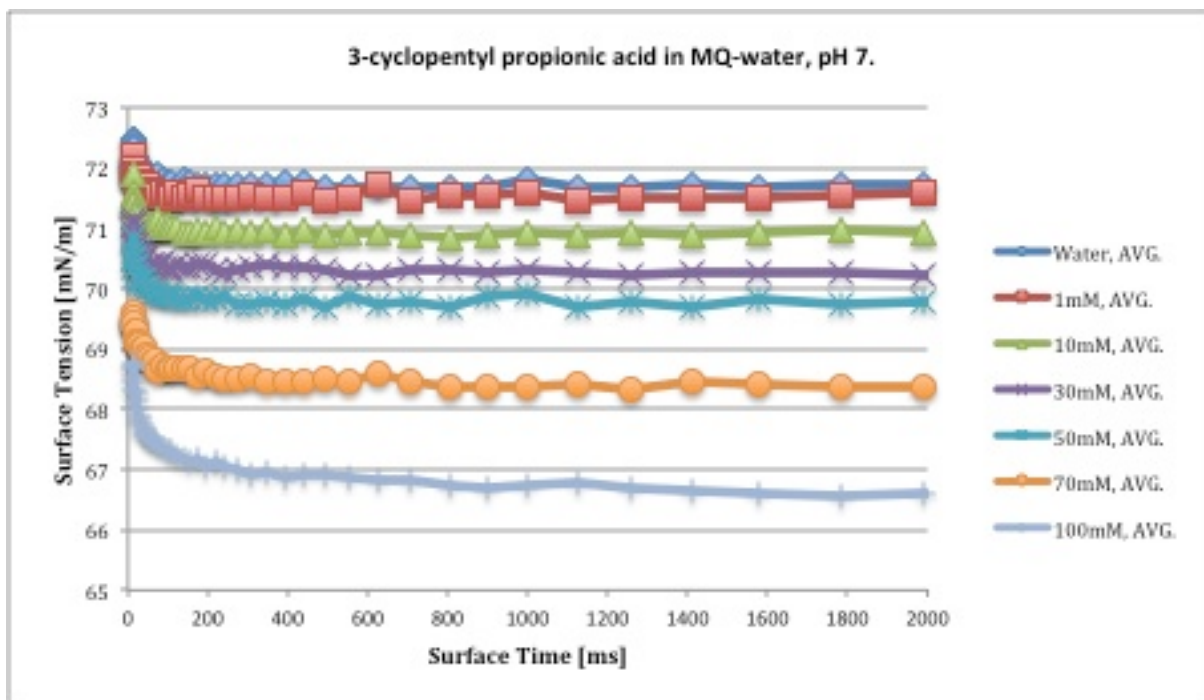


Figure 20: The figure shows the measured interfacial tension for 3-cyclopentyl propionic acid at different concentrations.

4.3 Influence of pH

The pH of the solutions is adjusted by addition of either HCL or NaOH. The adjustment of the pH will affect the solutions in different ways. The figures below display how the surface tension changes according to pH for three different concentrations in both MQ-water and in synthetic brine. In the plots below the choice of concentrations was made to include a low, a medium and a high value of the overall concentrations spectra. Throughout the plots the same concentration with different pH values are presented with similar colours. For all pH values see Appendix A.

Figure 21 represents Pyridine in MQ-water. Pyridine dissolved in MQ-water had a pH of 6,93 – 8,75 before adjustment. The pH increased with concentration. In the figure the plots after pH adjustments are plotted. These plots show that for pH 7 and pH 10 the concentration is the only thing affecting the interfacial tension. The measurements for pH 2 differ from the results at pH 7 and pH 10. The measurements for Pyridine at pH 2 exhibit only small changes in the interfacial tension for all the concentrations, which indicates that the low pH influence the adsorption on the interface. The behaviour for Pyridine at pH 2 is described further in chapter 4.5 *Pyridine at pH 2*.

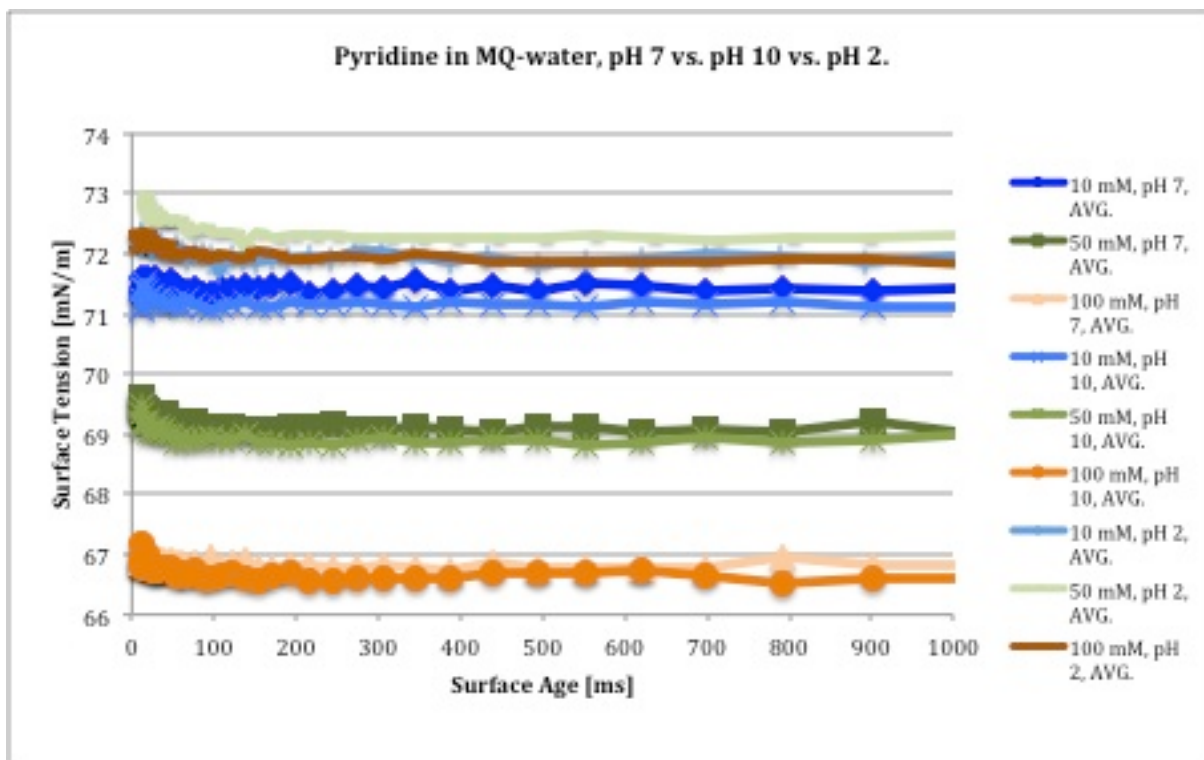


Figure 21: The figure shows the influence of pH on the interfacial tension of Pyridine.

Figure 22 represents Phenol in MQ-water. Phenol dissolved in MQ-water had a pH range between 5,20 – 5,76 before adjustment. The pH values do not change consistently with concentration, but the general trend indicates a decrease in pH with increasing concentration. As seen in the figure the pH affects the adsorption to the surface and therefore the interfacial tension. At the lowest concentration the pH seems to have no effect, 10 mM at the different pH values is presented with three different blue colours, and as observed the surface tension exhibits only small variations.

The measurements for 50 mM at the different pH values are described using a variation of green colours, and here a variation with pH is observed. The interfacial tension measured at pH 10 exhibits a considerably higher value than the measured values at pH 2 and pH 7, which only exhibits slight differences in the measured values. This indicates that Phenol is more surface active at lower pH values, and that the amount of added 1 M NaOH therefore influences the adsorption of Phenol on the interface.

The measurements for 100 mM at the different pH values are presented with different turquoise colours. The trend is similar when comparing with the measurements for 50 mM, but the differences at 100 mM are more severe than for 50 mM. The measured values for interfacial tension at pH 10 are significantly higher than the values measured for pH 2 and pH 7, which indicate the Phenol is more surface active at lower pH. As seen in the figure the values for interfacial tension for the lower pH values are similar, and vary with around 1 mN/m.

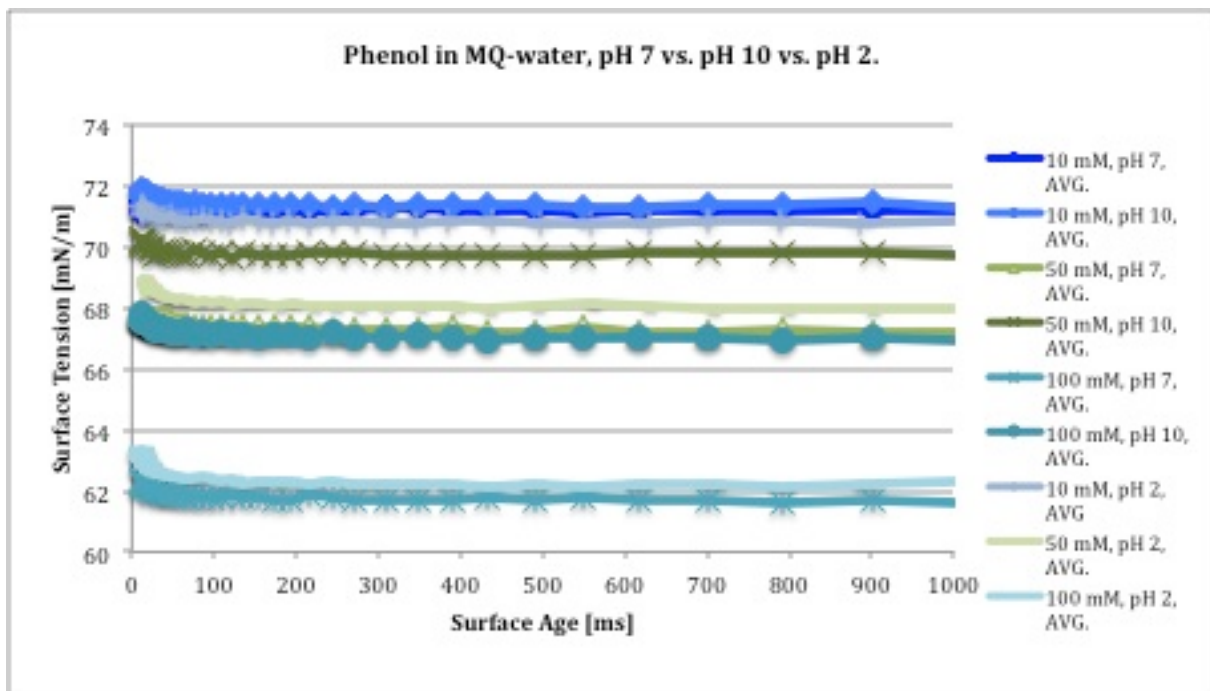


Figure 22: The figure shows the influence of pH on the interfacial tension of Phenol.

Figure 23 represents the measured surface tension plotted against surface age for 3-cyclopentyl propionic acid. The pH of the acid in MQ-water is $3,28 \pm 0,5$. As seen in the figure pH has an affect on the surface tension for the lower and the higher concentrations. Since the chemical was insoluble at pH 2 the figure only contains the measurements at pH 7 and pH 10. The difference between the two pH values with concentration 10 mM are around 1 mN/m, which indicates that the solution follow the same pattern and the pH is the consequence of the slight change in surface tension. The results for 50 mM at pH 7 and 10 display no differences between the two measurements, which implies that pH does not affect the concentration in the same manner. For 100 mM the decrease in surface tension is largest for pH 7 and the difference between the

two are larger than for 10 mM. This indicates that the acid will affect the surface tension more at pH values below 7.

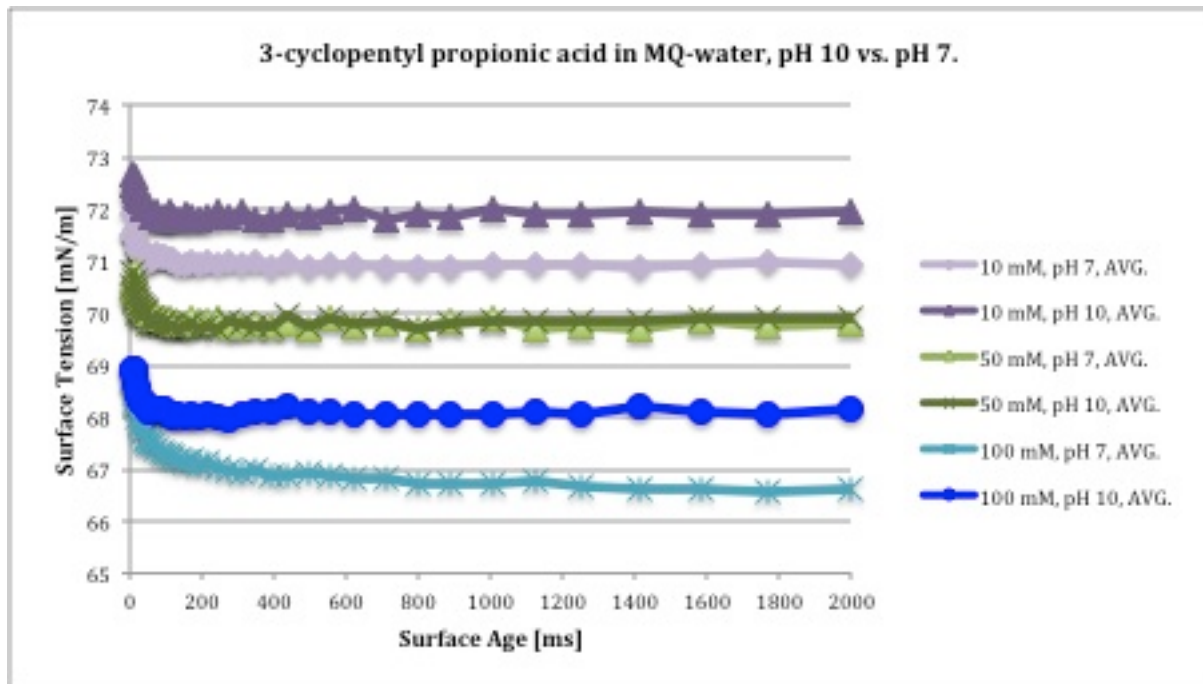


Figure 23: The figure shows the influence of pH on the interfacial tension of 3-cyclopentyl propionic acid.

In synthetic brine only pH 2 and pH 7 are measured, due to precipitation at pH 10. The surface tension for 10 mM, 50 mM and 100 Mm Pyridine at pH 2 and pH 7 in synthetic brine is presented in figure 24. The synthetic brine makes the pH of the solution obtain a neutral value equal to $7,2 \pm 0,5$ for all the concentration, compared to an increase in pH with concentration in MQ-water. This is because of the presence of electrolytes in solution, which contributes to neutralization of the molecules present. The same situation occurs in the brine as in the MQ-water, as mentioned previous in the results. The surface tension in the brine and in the MQ-water at pH 7 exhibits only minor differences. The behaviour of Pyridine at pH 2 is further discussed in chapter 4.5 *Pyridine at pH 2.*

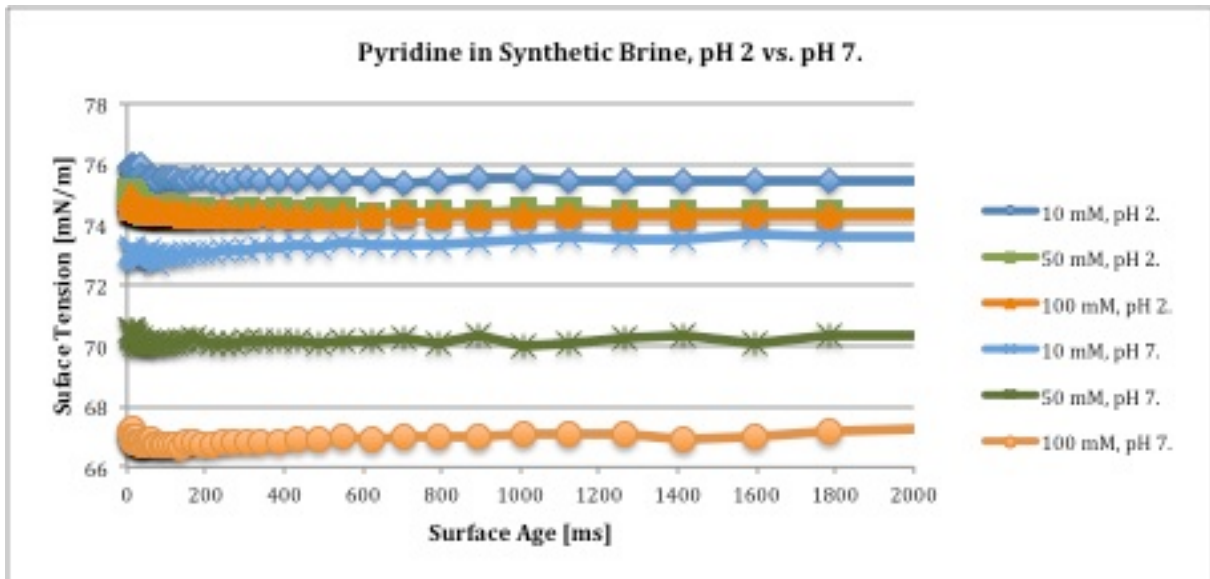


Figure 24: The figure shows the influence of pH on the interfacial tension of Pyridine in synthetic brine.

The results of the influence of pH on Phenol in synthetic brine are presented in figure 25. Here it is clearly observed that the pH values of the solution do not affect the interfacial tension. The values of the pH in the solutions of Phenol were neutral with values between 7,10 – 7,41, which is a change from Phenol in MQ-water indicating that the electrolytes present in the synthetic brine affects the pH of the solutions. The surface tension measurements are however not affected by changes in the pH. As displayed in the figure the surface tension of Phenol in synthetic brine only exhibits minute changes with pH and can be considered equal.

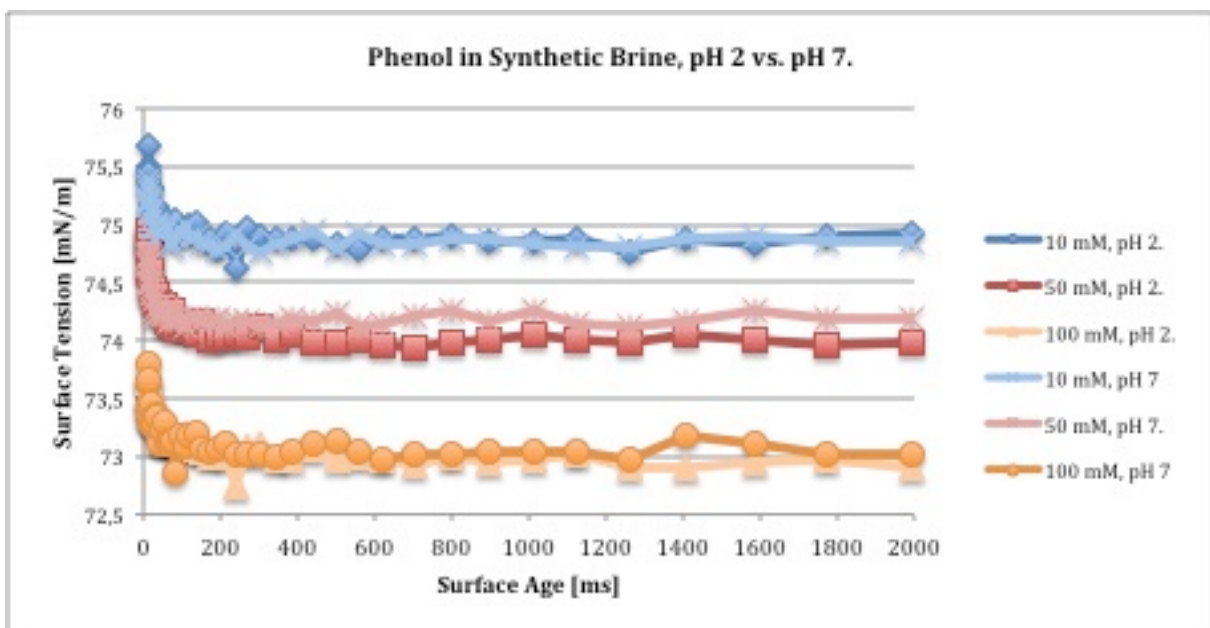


Figure 25: The figure shows the influence of pH on the interfacial tension of Phenol.

4.4 Influence of Synthetic Brine

Synthetic brine consists of dissolved salts. In figure 26 the surface tension of the solvents are presented in order to show the difference in surface tension. As seen in the figure the surface tension of the MQ-water and the synthetic brine differs with approximately 3 mN/m. The difference may occur because the electrolytes are repelled from the interface due to electrostatic repulsive forces that occur at the interface [37]. Another phenomenon that needs attention is that at the interface the hydration of ions can create an ion-free layer, which leads to an increase in surface tension [37].

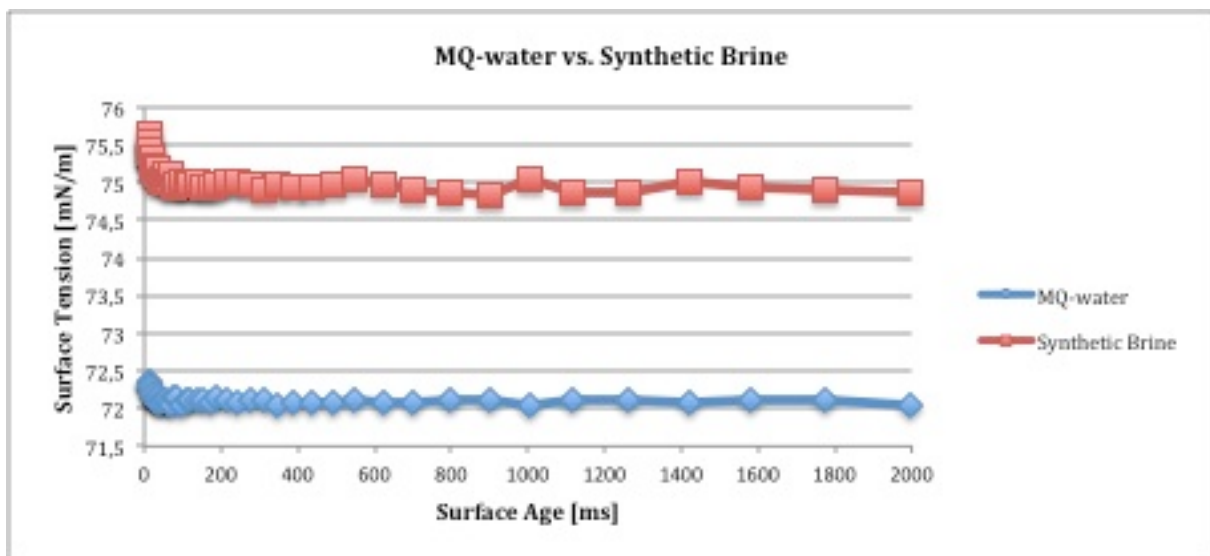


Figure 26: The figure shows the difference in interfacial tension for the solvents MQ-water and synthetic brine.

The salinity of the solution may affect the surface properties by introducing the salting out effect. The salting out effect influences the solubility of the chemicals in solution by binding the water molecules causing dehydration of the system.

In figure 27 the influence of synthetic brine is described using Pyridine with three different concentrations at pH 7. Pyridine is a highly soluble compound and exhibits high solubility in both MQ-water and in synthetic brine. As seen in the figure an increase in concentration reduces the difference between the solutions. The surface tension for 100 mM Pyridine in synthetic brine and in MQ-water displays similarities. This indicates that at high concentrations Pyridine is equally surface active in both MQ-water and

synthetic brine, but as the concentration decreases the difference in surface tension increases. Overall, in synthetic brine the surface activity of Pyridine is reduced.

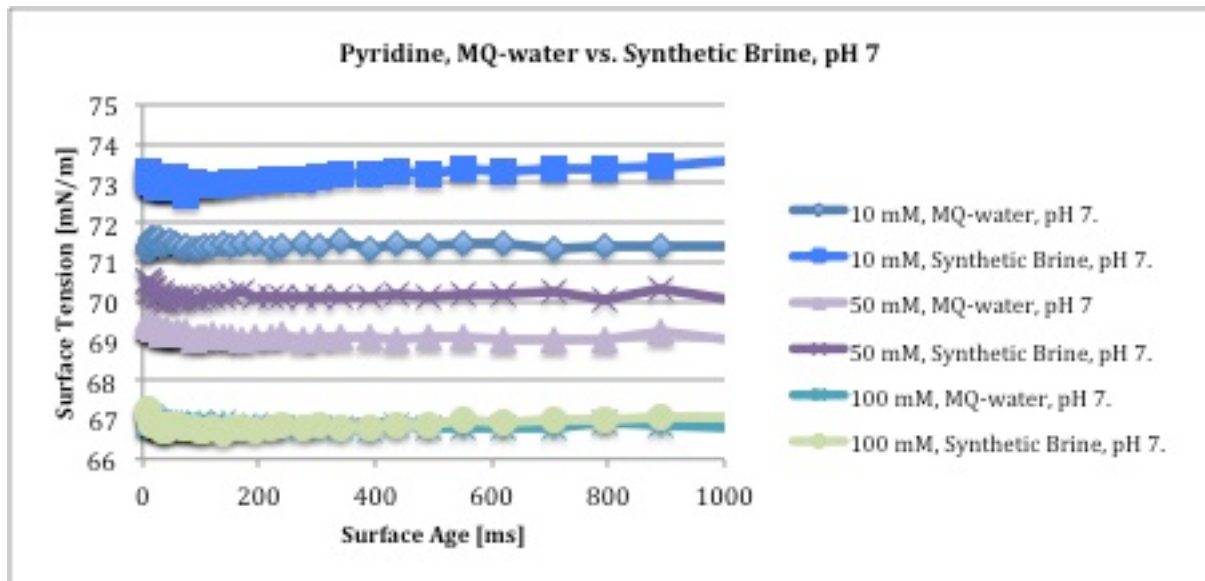


Figure 27: The figure shows the influence of synthetic brine on three different concentrations of Pyridine at pH 7.

The influence of synthetic brine on Phenol is described by figure 28. As presented in the figure the influence is significant. In synthetic brine the surface tension exhibits only small changes compared to the surface tension in the MQ-water. This indicates that the ions in the synthetic brine are competing with the Phenol for a place on the interface, causing some of the dissolved phenol molecules to be repelled from the surface. The surface activity of Phenol is reduced in the synthetic brine.

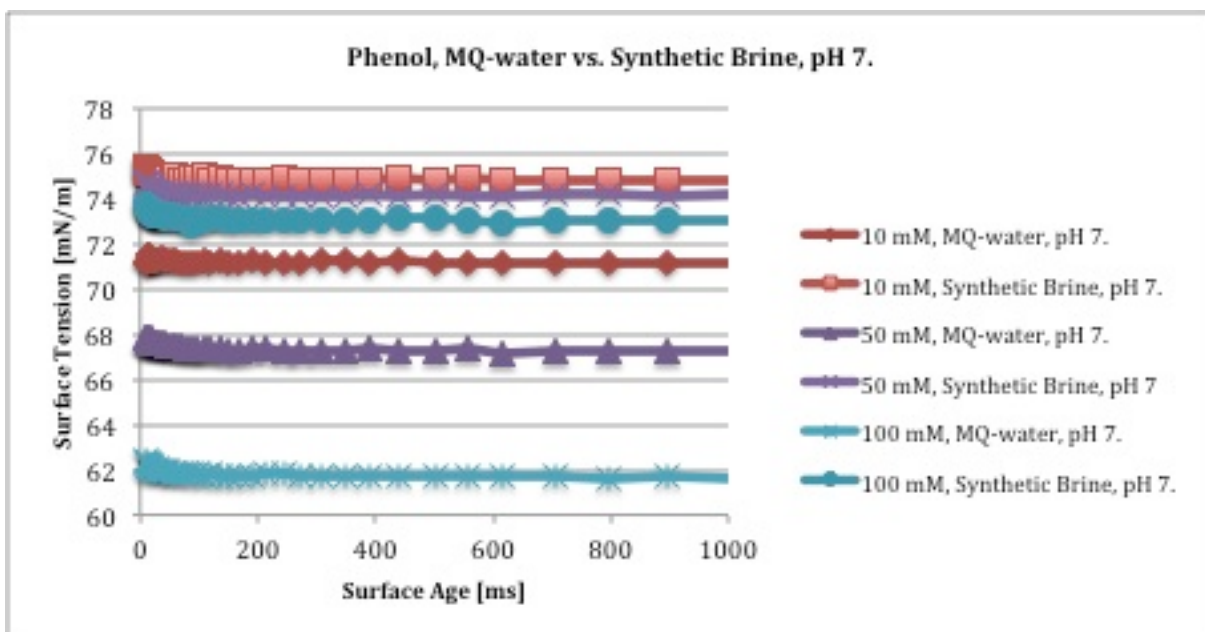


Figure 28: The figure shows the influence of synthetic brine on three different concentrations of Phenol at pH 7.

Figure 29 is added to describe the difference in surface tension for the three chemicals used throughout this thesis. The 3-cyclopentyl propionic acid has the slowest adsorption compared to Pyridine and Phenol. Phenol has the lowest surface tension and is considered to be the most surface active.

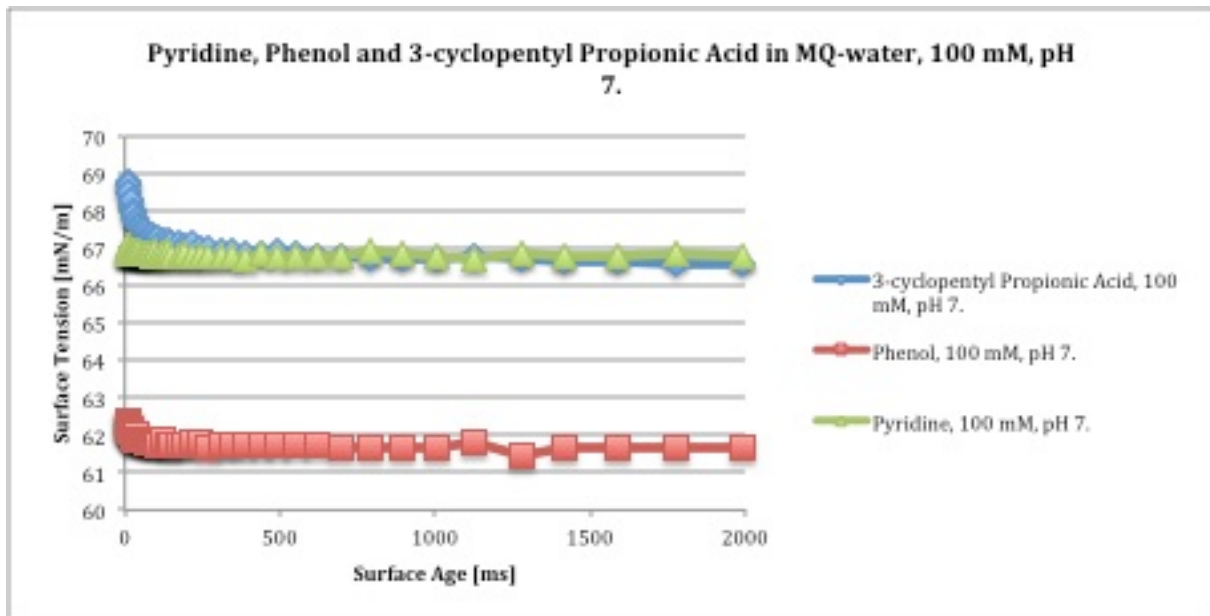


Figure 29: The figure describes the variation in surface tension for the three chemicals used in this thesis.

4.5 Pyridine at pH 2

Pyridine in MQ-water and in synthetic brine differs from the general trends throughout these results and are therefore discussed in detail here.

Figure 30 represents Pyridine in MQ-water. This figure clearly indicates that the Pyridine is affected by the low pH. The interfacial tension exhibits only small variation for all six concentrations, and the measurements all lay around the interfacial tension of MQ-water at 72 mN/m. The interval where the variations appear in the range from 73 mN/m to 71,8 mN/m, which means that the overall change in interfacial tension from 1 mM to 100 mM is 1,2 mN/m. The adjustment of the pH too pH 2 is done by addition of 1 M HCl to each concentration. The acid may influence the molecule by reacting with the lone pair of electrons on the nitrogen atom in the benzene ring of pyridine. In water Pyridine exhibits Bronsted-base properties, meaning that the addition of more H⁺ will

make the solution present as a highly soluble acid. Highly soluble acids like this shows low affinity to the surface and prefers to be in the bulk solution.

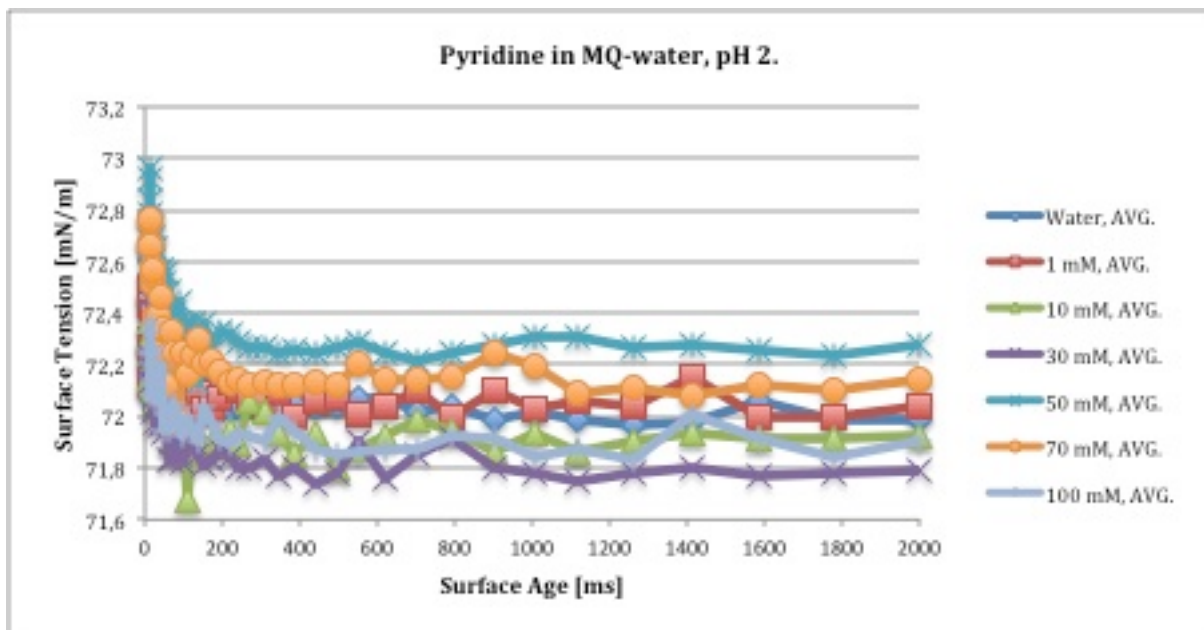


Figure 30: The figure shows the relationship between interfacial tension and surface age for Pyridine at pH 2 in MQ-water.

The low affinity to the surface is clearly observed in the figures. In figure 31 the surface tension is plotted against surface age for Pyridine in synthetic brine. The same trends are observed in this figure compared to the figure above. The general increase in surface tension is due to added electrolytes. The slight difference between 1 mM and 100 mM in synthetic brine can be due to reduction in repulsion between charged surface active molecules at the interface.

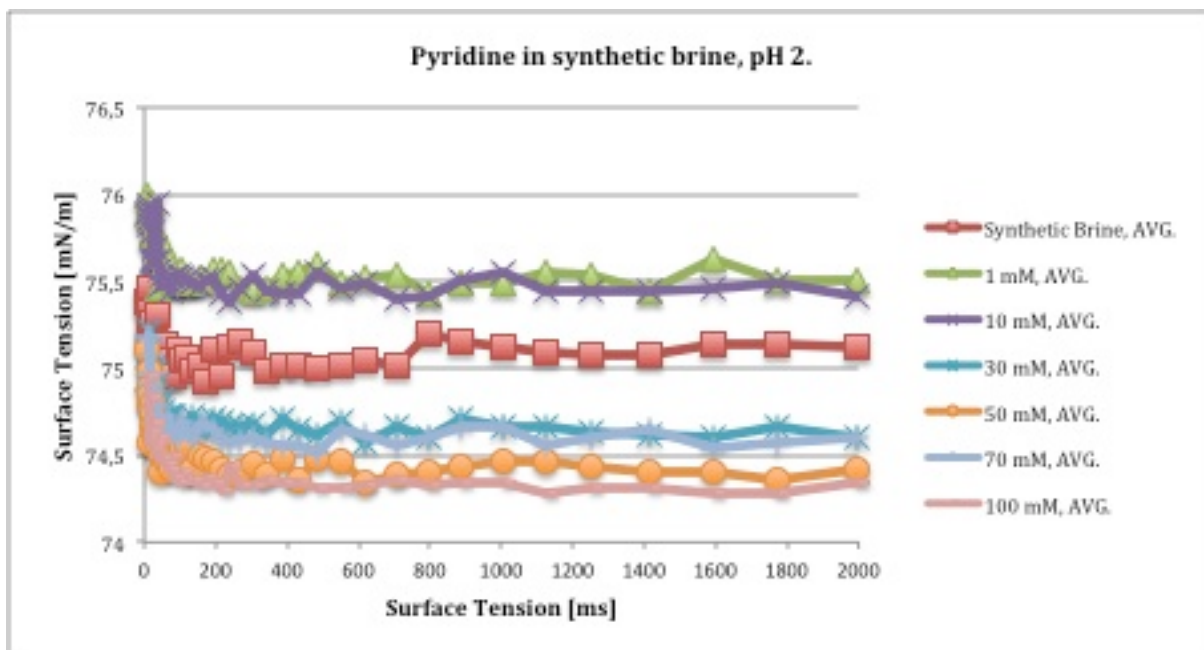


Figure 31: The figure shows the relationship between interfacial tension and surface age for Pyridine at pH 2 in synthetic brine.

4.6 Gibbs Adsorption Isotherm

The Gibbs Adsorption Isotherm plots and the calculations of the surface excess describe if the surfactants adsorb or desorb in solution. If the calculated surface excess has a positive prefix the surfactants adsorb on the interface, and if the prefix is negative the surfactants desorb back to the bulk. For a surfactant solution in equilibrium the surface excess is the interfacial concentration of a surfactant [29].

Figure 32 represent the Gibbs Adsorption Isotherm plot for Pyridine in MQ-water. The plot for Pyridine at pH 2 shows a clear deviation from linearity, R^2 . The results are ok, but cannot be used due to low adsorption. The reason for the low value may be related to the small variation in the interfacial tension at this pH, which may indicate zero adsorption on the surface. For pH 7 and pH 10 the plots are nearly identical and the linear relationship shows almost no deviation.

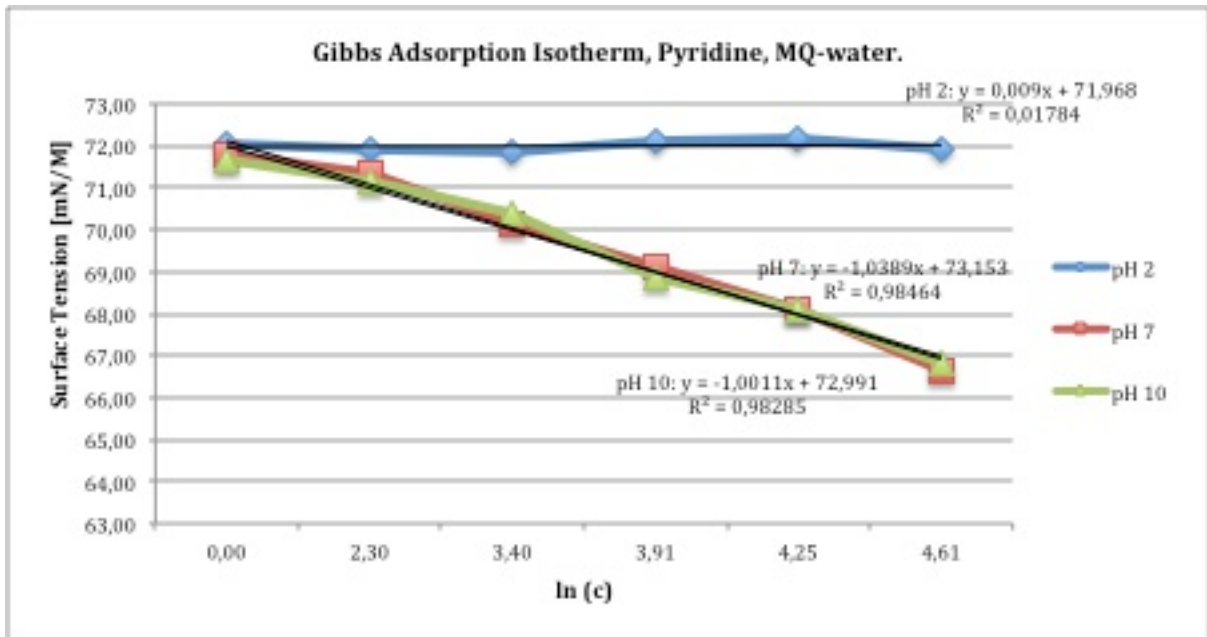


Figure 32: The figure shows the plot of surface tension versus $\ln(c)$ and the corresponding linear relationship.

Table 3 displays the calculated values for the surface excess for Pyridine in MQ-water. The calculated values for pH 7 and pH 10 are similar. The values indicate that the Pyridine molecules adsorb on the surface and that the surface excess of pyridine in MQ-water is not dependent on pH over a certain value. The surface excess of Pyridine at pH 2 can be neglected since the deviation from linearity is large, but in general negative values of surface excess indicates desorption from interface into the bulk.

Table 3: The table shows the values for surface excess for pyridine at different pHs.

pH	Surface Excess
2	$-3,63 \cdot 10^{-6}$
7	$4,2 \cdot 10^{-4}$
10	$4,04 \cdot 10^{-4}$

The plot for Gibbs Adsorption Isotherm for Pyridine in synthetic brine is presented in figure 33. Also in this figure the deviation from linearity is lower than 0,80 for Pyridine at pH 2. The variation in concentrations for Pyridine at pH 2 in synthetic brine and in MQ-water is low. Low pH clearly is affecting the Pyridine molecule. For pH 7 the plot is linear with a value of R^2 equal to 0,99461.

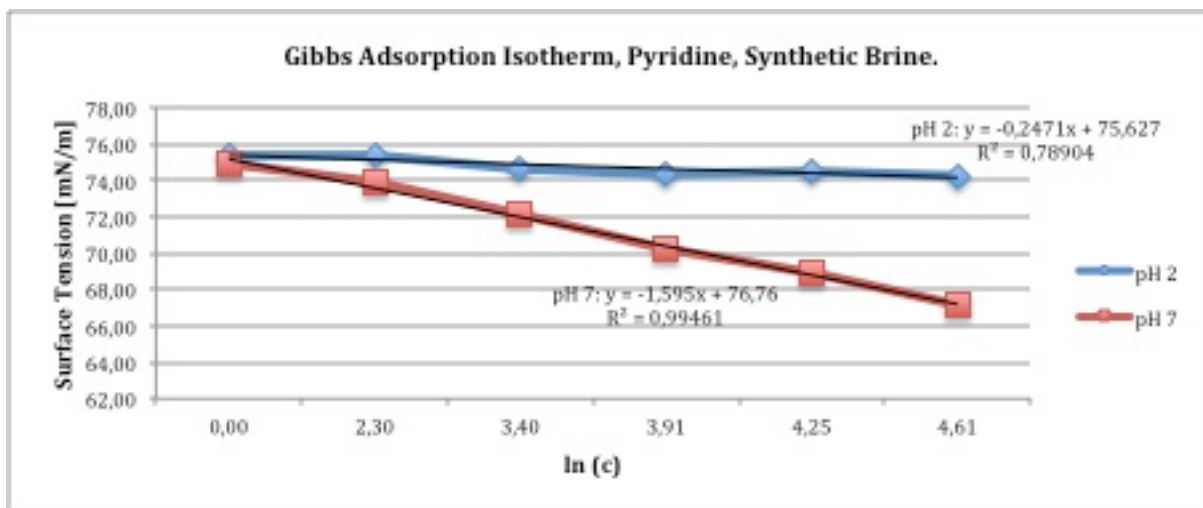


Figure 33: The figure shows the plot of surface tension versus ln (c) and the corresponding linear relationship.

Table 4 represents the values of surface excess related to the figure above. The values indicate adsorption on the interface.

Table 4: The table shows the values for surface excess for pyridine at different pHs.

pH	Surface Excess
2	$9,97 * 10^{-5}$
7	$6,44 * 10^{-4}$

When comparing the calculated values for surface excess at pH 7 in MQ-water and synthetic brine an increase in surface excess is found. This increase is due to the salting out effect.

Figure 34 shows the adsorption isotherm for Phenol in MQ-water. The deviation from linearity in the three plots is above the lower limit, and all the measurements are valid. The plots for pH 2, pH 7 and pH 10 are nearly identical at low concentrations, but at higher concentrations pH 10 differs from the lower pHs.

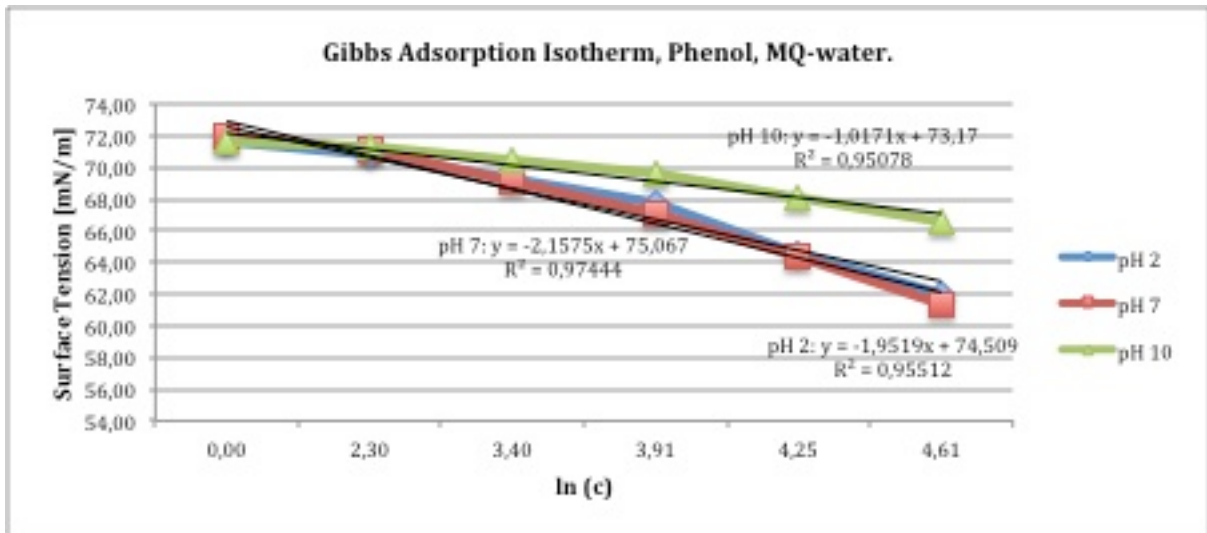


Figure 34: The figure shows the plot of surface tension versus $\ln(c)$ and the corresponding linear relationship.

Table 5 displays the values of surface excess. The values express adsorption at all the pHs, but at pH 2 and pH 7 the surface excess is larger. This indicates that the adsorption of Phenol is more extensive at pH 7 and pH lower than pH 7. The surface excess at pH 2 and pH 7 displays some variations, but when comparing the value for pH 10 the difference between surface excess for pH 2 and pH 7 quite small. Overall, there is more adsorption at lower pH.

Table 5: The table shows the values for surface excess for pyridine at different pHs.

pH	Surface Excess
2	$7,88 * 10^{-4}$
7	$8,71 * 10^{-4}$
10	$4,11 * 10^{-4}$

Figure 35 is presented below and shows the plots for Phenol in synthetic brine. The deviation from linearity is greater than 0,85. The graphs are nearly identical at low concentrations, but at elevated concentrations pH 7 differs from pH 2.

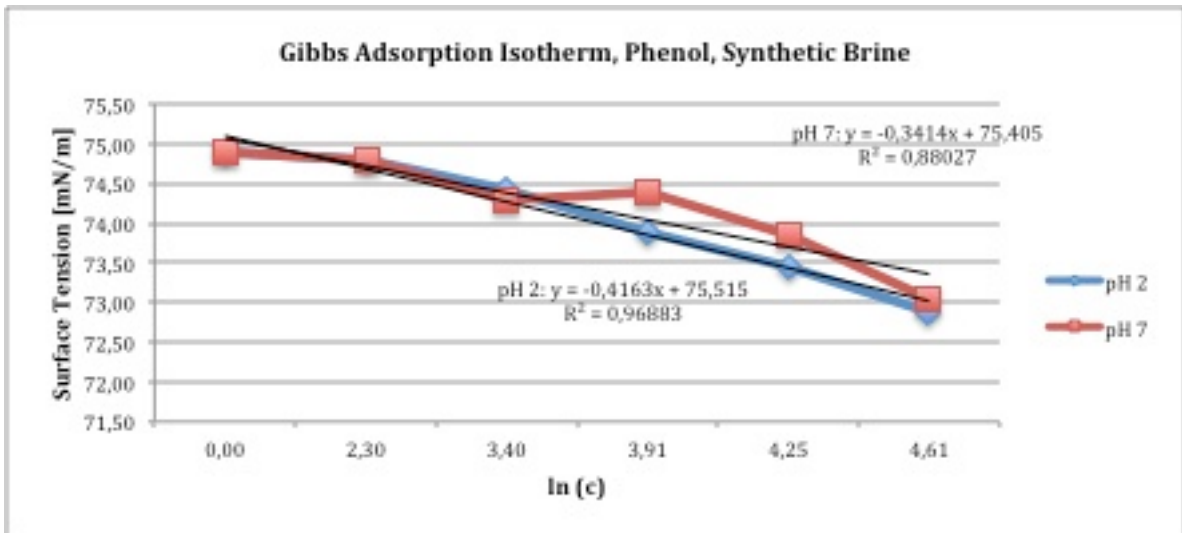


Figure 35: The figure shows the plot of surface tension versus $\ln (c)$ and the corresponding linear relationship.

The values presented in table 6 describe the surface excess of Phenol in synthetic brine. The calculated values show small variation for the different pH, which indicates that surface excess of Phenol in synthetic brine is not pH dependant.

Table 6: The table shows the values for surface excess for pyridine at different pHs.

pH	Surface Excess
2	$1,68 \cdot 10^{-4}$
7	$1,38 \cdot 10^{-4}$

When comparing the surface excess values for Phenol in MQ-water and synthetic brine it is clear that the salt composition of the brine affects the surface excess of Phenol. The lowering in values for excess indicates that Phenol is more surface active in MQ-water than in synthetic brine.

The Gibbs Adsorption Isotherm presented in figure 36 is the plot for 3-cyclopentyl propionic acid. The plot display similar trends for the two pH values, which should indicate that the values for the surface excess are similar.

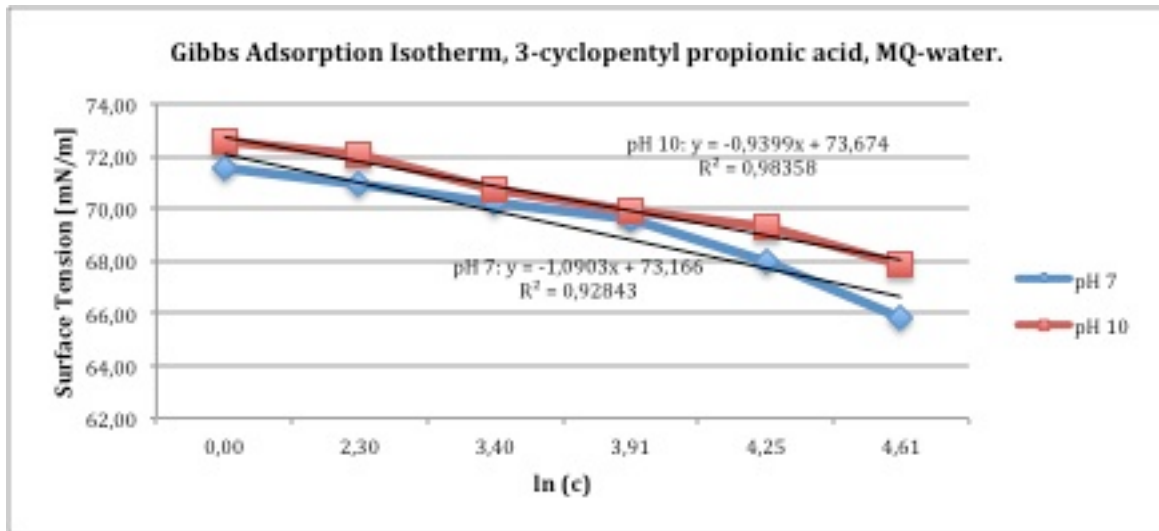


Figure 36: The figure shows the plot of surface tension versus $\ln(c)$ and the corresponding linear relationship.

The values for surface excess of 3-cyclopentyl propionic acid are shown in table 7, and as the graph predicted the values are similar.

Table 7: The table shows the values for surface excess for pyridine at different pHs.

pH	Surface Excess
7	$4,40 \cdot 10^{-4}$
10	$3,79 \cdot 10^{-4}$

Calculations of the surface excess are shown in Appendix B.

4.7 Diffusion Coefficient; Diffusion Controlled or Mixed-Kinetic Diffusion Controlled

The plots and the calculations of diffusion coefficients are done in order to determine if the adsorption to the interface is diffusion-controlled or controlled by mixed-kinetic diffusion. The determination gives knowledge about how the molecules adsorb on the interface, either by direct adsorption or by adsorption after breaking an energy barrier. As mentioned in the theory the calculations of the diffusion coefficient is dependant on the form of the surface that the molecules adsorb on and the linearity of the plot. The equations used to calculate the coefficients are based on the assumption that the interface is clean when the bubbles are formed and that the molecules adsorb as the time passes.

A description on how the surface tension act when a clean interface is formed before adsorption is presented in figure 37.

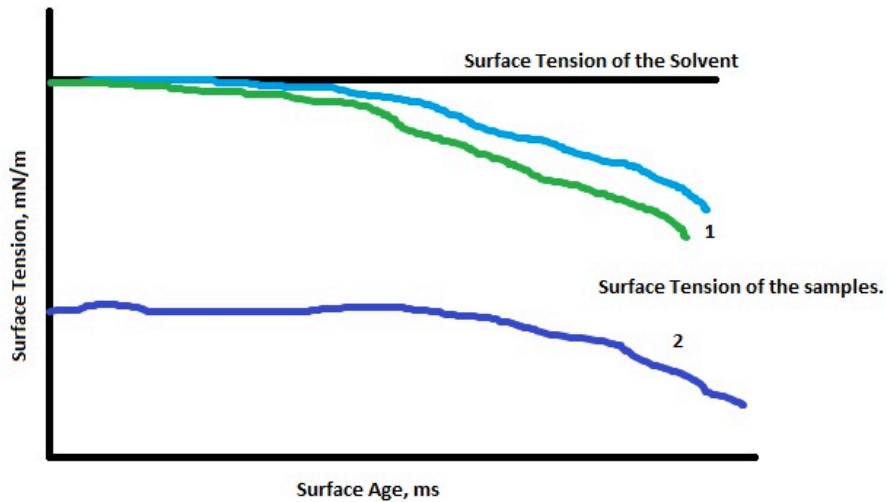


Figure 37: 1) Represent a clean interface before molecules adsorb, 2) shows the case where molecules have adsorbed as soon as the interface was formed.

As displayed in the figure the surface tension of the solutions needs to be similar to the surface tension of the solvent for the equations of the diffusion coefficient to be valid, as seen in the graphs marked with (1). In measurements done in this thesis all the results indicated adsorption as soon as the interface is formed, which is similar to the situation represented in the graph with the number (2). This indicates that a clean interface does not exist and the equations used to calculate the diffusion coefficients are invalid.

To distinguish between diffusion controlled adsorption and adsorption controlled by mixed-kinetic diffusion the time scale of the adsorption is important. For adsorption controlled by mixed-kinetic diffusion the time scale is larger than for diffusion controlled adsorption. This is because of an adsorption barrier, which can be related to a number of things including reorientation of the surfactant, number of vacant sites and the potential energy of the system. Diffusion controlled adsorption is faster, because the adsorption from the subsurface occurs immediately after the diffusion from the bulk to the subsurface.

5 Conclusion

Throughout this thesis three chemicals with different properties, concentrations and various pH have been used. Each chemical shows different behaviour in both MQ-water and synthetic brine. Pyridine shows similar behaviour for all the six concentrations at pH 2 in both MQ-water and synthetic brine compared to the other pH values. For pH 7 and pH 10 the influence of concentration is more severe. The influence of pH at the higher pH values is almost non-existing for Pyridine in MQ-water. For Phenol in MQ-water an increase in concentration will lead to a decrease in surface tension. The influence of pH on Phenol indicates that at lower pH values Phenol is more surface active. For Phenol in synthetic brine the changes in pH has no effect on the surface tension. When comparing the result for Phenol in synthetic brine and MQ-water it is clear that the surface activity of Phenol decreases in synthetic brine, leading to more severe decrease in surface tension in MQ-water than in synthetic brine. For 3-cyclopentyl propionic acid the influence of concentration on surface tension is clear. The decrease in surface tension before equilibrium values are reached is larger for this acid. The surface tension for this acid seems to be dependent on pH at low and at high concentrations.

The 3-cyclopentyl propionic acid has the slowest adsorption compared to Pyridine and Phenol. Phenol has the lowest surface tension and is considered to be the most surface active.

6 Further Work

The number of chemicals investigated can be extended to for example include a sulphur-containing compound.

6 References

1. Moulijn, J.A., M. Makkee, and A. van Diepen, *Chemical Process Technology*. 2001: John Wiley.
2. *Quintiq - Solving the World's Planning Puzzles*, in *Oil & Gas*
<http://www.quintiq.com/industries/oil-and-gas-planning.html>.
3. Speight, J.G., *The Chemistry and Technology of Petroleum, Fifth Edition*. 2014: Taylor & Francis.
4. Read, A.D. and R.A.A. Blackman, *Oily water discharges from offshore North Sea installations: A perspective*. *Marine Pollution Bulletin*, 1980. **11**(2): p. 44-47.
5. Ray, J.P. and F.R. Engelhardt, *Produced Water: technological, environmental issues and solutions ; [proceedings of the 1992 International Produced Water Symposium, held February 4 - 7, 1992, in SanDiego, California]*. 1992: Plenum Press.
6. Eftekhardadkhan, M. and G. Øye, *Dynamic Adsorption of Organic Compounds Dissolved in Synthetic Produced Water at Air Bubbles: The Influence of the Ionic Composition of Aqueous Solutions*. *Energy & Fuels*, 2013. **27**(9): p. 5128-5134.
7. Stewart, M. and K. Arnold, *Emulsions and oil treating equipment: selection, sizing and troubleshooting*. 2008: Gulf Professional Publishing.
8. Fakhru'l-Razi, A., et al., *Review of technologies for oil and gas produced water treatment*. *Journal of Hazardous Materials*, 2009. **170**(2-3): p. 530-551.
9. *Norsk Olje og Gass. Olje- og gassindustrien jobber kontinuerlig for å redusere utslippene til havet fra offshorevirksomheten.*, in *Havmiljø*. *Norsk olje & gass*:
<http://www.norskoljeoggass.no/no/faktasider/Miljo1/havmiljo/>.
10. Neff, J.M., *Bioaccumulation in Marine Organisms: Effect of Contaminants from Oil Well Produced Water*. 2002: Elsevier Science.
11. Shi, Q., et al., *Characterization of Heteroatom Compounds in a Crude Oil and Its Saturates, Aromatics, Resins, and Asphaltenes (SARA) and Non-basic Nitrogen Fractions Analyzed by Negative-Ion Electrospray Ionization Fourier Transform Ion Cyclotron Resonance Mass Spectrometry*. *Energy & Fuels*, 2010. **24**(4): p. 2545-2553.
12. Stanford, L.A., et al., *Identification of Water-Soluble Heavy Crude Oil Organic-Acids, Bases, and Neutrals by Electrospray Ionization and Field Desorption Ionization Fourier Transform Ion Cyclotron Resonance Mass Spectrometry*. *Environmental Science & Technology*, 2007. **41**(8): p. 2696-2702.
13. Robinson, D., *Oil and gas: Water treatment in oil and gas production – does it matter?* *Filtration & Separation*, 2010. **47**(1): p. 14-18.
14. Prescott, N., et al., *Treating and Releasing Produced Water at the Ultradeepwater Seabed*.
15. Robinson, D., *Oil and gas: Treatment of produced waters for injection and reinjection*. *Filtration + Separation*, 2013. **50**(4): p. 36-43.
16. Strickland, W.T., Jr., *Laboratory Results of Cleaning Produced Water by Gas Flotation*.
17. Mooaal, R., *Oily wastewater cleanup by gas flotation*. 2002.

18. Moosai, R. and R.A. Dawe, *Gas attachment of oil droplets for gas flotation for oily wastewater cleanup*. Separation and Purification Technology, 2003. **33**(3): p. 303-314.
19. Oliveira, R.C.G., G. Gonzalez, and J.F. Oliveira, *Interfacial studies on dissolved gas flotation of oil droplets for water purification*. Colloids and Surfaces A: Physicochemical and Engineering Aspects, 1999. **154**(1-2): p. 127-135.
20. Eftekhardadkhah, M., *Interfacial properties of dissolved crude oil components in produced water*, in Department of Chemical Engineering
. 2013, NTNU: <http://urn.kb.se/resolve?urn=urn:nbn:no:ntnu:diva-23900>.
21. Holmberg, K., et al., *Introduction to Surfactants*, in *Surfactants and Polymers in Aqueous Solution*. 2003, John Wiley & Sons, Ltd. p. 1-37.
22. Holmberg, K., et al., *Surfactant Micellization*, in *Surfactants and Polymers in Aqueous Solution*. 2003, John Wiley & Sons, Ltd. p. 39-66.
23. McElroy, N.R. and P.C. Jurs, *Prediction of Aqueous Solubility of Heteroatom-Containing Organic Compounds from Molecular Structure*. Journal of Chemical Information and Computer Sciences, 2001. **41**(5): p. 1237-1247.
24. Mitchell, B.E. and P.C. Jurs, *Prediction of Aqueous Solubility of Organic Compounds from Molecular Structure*. Journal of Chemical Information and Computer Sciences, 1998. **38**(3): p. 489-496.
25. Turner, A., *Salting out of chemicals in estuaries: implications for contaminant partitioning and modelling*. Science of The Total Environment, 2003. **314-316**(0): p. 599-612.
26. Xie, W.-H., W.-Y. Shiu, and D. Mackay, *A review of the effect of salts on the solubility of organic compounds in seawater*. Marine Environmental Research, 1997. **44**(4): p. 429-444.
27. Neff, J., K. Lee, and E. DeBlois, *Produced Water: Overview of Composition, Fates, and Effects*, in *Produced Water*, K. Lee and J. Neff, Editors. 2011, Springer New York. p. 3-54.
28. Mørk, P.C., *Overflate og kolloidkjemi: grunnleggende prinsipper og teorier*. 1999, Trondheim: Norges teknisk-naturvitenskapelige universitet, Institutt for kjemisk prosessteknologi. XII, 307 s. ill.
29. Eastoe, J. and J.S. Dalton, *Dynamic surface tension and adsorption mechanisms of surfactants at the air-water interface*. Advances in Colloid and Interface Science, 2000. **85**(2-3): p. 103-144.
30. Liu, J. and U. Messow, *Diffusion-controlled adsorption kinetics at the air/solution interface*. Colloid and Polymer Science, 2000. **278**(2): p. 124-129.
31. Tadros, T., *Gibbs Adsorption Isotherm*. Encyclopedia of Colloid and Interface Science, 2013: p. 626-626.
32. Eftekhardadkhah, M., P. Reynders, and G. Øye, *Dynamic adsorption of water soluble crude oil components at air bubbles*. Chemical Engineering Science, 2013. **101**(0): p. 359-365.
33. Ikeda, S., M.-A. Tsunoda, and H. Maeda, *The application of the Gibbs adsorption isotherm to aqueous solutions of a nonionic-cationic surfactant*. Journal of Colloid and Interface Science, 1978. **67**(2): p. 336-348.
34. Liu, J., C. Wang, and U. Messow, *Adsorption kinetics at air/solution interface studied by maximum bubble pressure method*. Colloid and Polymer Science, 2004. **283**(2): p. 139-144.

35. Li, X., et al., *A simple numerical solution to the Ward–Tordai equation for the adsorption of non-ionic surfactants*. *Computers & Chemical Engineering*, 2010. **34**(2): p. 146-153.
36. Holmberg, K., et al., *Surface Tension and Adsorption at the Air–Water Interface*, in *Surfactants and Polymers in Aqueous Solution*. 2003, John Wiley & Sons, Ltd. p. 337-355.
37. Ohshima, H. and H. Matsubara, *Surface tension of electrolyte solutions*. *Colloid and Polymer Science*, 2004. **282**(9): p. 1044-1048.
38. Farooq, U., et al., *Interfacial Tension Measurements Between Oil Fractions of a Crude Oil and Aqueous Solutions with Different Ionic Composition and pH*. *Journal of Dispersion Science and Technology*, 2013. **34**(5): p. 701-708.
39. Fileti, E.E., et al., *Electronic changes due to thermal disorder of hydrogen bonds in liquids: Pyridine in an aqueous environment*. *Physical Review E*, 2003. **67**(6): p. 061504.
40. Fainerman, V.B. and R. Miller, *Maximum bubble pressure tensiometry—an analysis of experimental constraints*. *Advances in Colloid and Interface Science*, 2004. **108–109**(0): p. 287-301.
41. *Bubble Pressure Method*. <http://www.kruss.de/services/education-theory/glossary/bubble-pressure-tensiometer/>.

List of Appendices

Appendix A

Appendix B

Appendix C

Appendix D

Appendix A: Mass Calculations and Measured Values for pH and Density

Mass Calculations:

Table A-1: Shows the molecular weight of the chemicals used.

Component	Structure	Molecular weight [g/mol]
Pyridine	C ₅ H ₅ N	79,09997
Phenol	C ₆ H ₆ O	94,111
3-cyclopentyl propionic acid	C ₅ H ₉ CH ₂ CH ₂ CO ₂ H	142,195

The mass is calculated with equation (1):

$$m = C * Mw * V \quad (A-1)$$

The solutions are diluted with the help of equation (2):

$$C_1 * V_1 = C_2 * V_2 \quad (A-2)$$

Table A-2: Shows concentration, pH and density for Pyridine in MQ-water.

Pyridine in MQ-water, pH 2.			
Concentration [mM]	Measured pH	Adjusted pH	Density [g/cm ³]
1	6,93	2,29	0,997328
1	6,99	2,23	0,997328
10	7,73	2,22	0,997406
10	7,78	2,19	0,997406
30	8,19	2,30	0,997803
30	8,20	2,23	0,997803
50	8,28	2,36	0,998175
50	8,50	2,21	0,998175
70	8,55	2,41	0,998536
70	8,55	2,29	0,998536
100	8,72	2,84	0,998987
100	8,73	2,55	0,998987

Table A-3: Shows concentration, pH and density for Pyridine in MQ-water.

Pyridine in MQ-water, pH 7.			
Concentration [mM]	Measured pH	Adjusted pH	Density [g/cm ³]
1	7,05	-	0,997750
1	7,03	-	0,997750
10	7,66	7,15	0,997766
10	7,70	7,16	0,997766
30	8,13	7,02	0,997144
30	8,17	7,07	0,997144
50	8,40	6,99	0,997138
50	8,41	7,05	0,997138
70	8,60	7,09	0,997184
70	8,50	7,09	0,997184
100	8,66	7,17	0,998002
100	8,66	7,17	0,998002

Table A-4: Shows concentration, pH and density for Pyridine in MQ-water.

Pyridine in MQ-water, pH 10.			
Concentration [mM]	Measured pH	Adjusted pH	Density [g/cm ³]
1	7,00	10,80	0,997062
1	7,05	10,81	0,997062
10	7,70	10,00	0,997050
10	7,80	10,09	0,997050
30	8,21	10,24	0,997098
30	8,19	10,28	0,997098
50	8,35	10,19	0,997135
50	8,38	10,24	0,997135
70	8,55	10,37	0,997178
70	8,49	10,36	0,997178
100	8,65	10,21	0,997243
100	8,68	10,27	0,997243

Table A-5: Shows concentration, pH and density of Pyridine in synthetic brine.

Pyridine in synthetic brine, pH 2.			
Concentration [mM]	Measured pH	Adjusted pH	Density [g/cm ³]
1	7,10	2,20	1,065532
1	7,07	2,14	1,065532
10	7,17	2,18	1,063892
10	7,20	2,09	1,063892
30	7,27	2,13	1,060718
30	7,26	2,18	1,060718
50	7,36	2,16	1,057862
50	7,32	2,20	1,057862
70	7,42	2,13	1,055428
70	7,40	2,01	1,055428
100	7,46	2,16	1,052195
100	7,48	2,02	1,052195
Brine	7,05	-	1,065967
Brine	7,05	-	1,065967

Table A-6: Shows concentration, pH and density of Pyridine in synthetic brine.

Pyridine in synthetic brine, pH 7.			
Concentration [mM]	Measured pH	Adjusted pH	Density [g/cm ³]
1	7,10	-	1,065678
1	7,09	-	1,065678
10	7,24	-	1,065759
10	7,21	-	1,065759
30	7,40	7,07	1,065608
30	7,35	6,99	1,065608
50	7,45	7,17	1,065422
50	7,44	7,15	1,065422
70	7,49	7,23	1,065485
70	7,44	7,20	1,065485
100	7,52	7,20	1,065150
100	7,51	7,18	1,065150
Brine	7,05	-	1,065781
Brine	7,05	-	1,065781

Table A-7: Shows concentration, pH and density of Phenol in MQ-water.

Phenol in MQ-water, pH 2.			
Concentration [mM]	Measured pH	Adjusted pH	Density [g/cm ³]
1	5,60	2,26	0,997167
1	5,63	2,19	0,997167
10	5,55	2,11	0,997327
10	5,53	2,03	0,997327
30	5,49	2,11	0,997439
30	5,41	2,12	0,997439
50	5,50	2,06	0,997630
50	5,78	2,11	0,997630
70	5,53	2,07	0,997788
70	5,41	2,10	0,997788
100	5,20	2,05	0,998033
100	5,41	2,02	0,998033

Table A-8: Shows concentration, pH and density of Phenol in MQ-water.

Phenol in MQ-water, pH 7.			
Concentration [mM]	Measured pH	Adjusted pH	Density [g/cm ³]
1	5,62	7,00	0,997048
1	5,65	7,10	0,997048
10	5,75	7,19	0,997124
10	5,76	7,35	0,997124
30	5,70	7,10	0,997269
30	5,65	7,09	0,997269
50	5,60	7,08	0,997435
50	5,75	7,10	0,997435
70	5,50	7,09	0,997607
70	5,56	7,08	0,997607
100	5,40	6,96	0,997878
100	5,41	7,15	0,997878

Table A-9: Shows concentration, pH and density of Phenol in MQ-water.

Phenol in MQ-water, pH 10.			
Concentration [mM]	Measured pH	Adjusted pH	Density [g/cm ³]
1	5,55	10,10	0,997085
1	5,65	10,30	0,997085
10	5,65	9,98	0,997339
10	5,85	10,01	0,997339
30	5,55	9,97	0,997902
30	5,65	9,94	0,997902
50	5,57	9,98	0,998520
50	5,53	9,97	0,998520
70	5,57	9,95	0,999021
70	5,60	9,94	0,999021
100	5,50	9,95	0,999938
100	5,50	9,94	0,999938

Table A-10: Shows concentration, pH and density of Phenol in synthetic brine.

Phenol in synthetic brine, pH 2.			
Concentration [mM]	Measured pH	Adjusted pH	Density [g/cm ³]
1	7,15	2,14	1,063984
1	7,09	2,14	1,063984
10	7,05	2,15	1,064162
10	7,06	2,12	1,064162
30	7,03	2,18	1,064176
30	7,06	2,20	1,064176
50	7,03	2,13	1,064136
50	7,09	2,06	1,064136
70	7,03	2,13	1,064147
70	7,04	2,07	1,064147
100	7,05	1,99	1,064006
100	7,02	2,10	1,064006
Brine	7,04	-	1,065334
Brine	7,04	-	1,065334

Table A-11: Shows concentration, pH and density of Phenol in synthetic brine.

Phenol in synthetic brine, pH 7.			
Concentration [mM]	Measured pH	Adjusted pH	Density [g/cm ³]
1	7,14	-	1,065365
1	7,09	-	1,065365
10	7,08	-	1,065473
10	7,08	-	1,065473
30	7,06	-	1,065509
30	7,06	-	1,065509
50	7,05	-	1,065508
50	7,05	-	1,065508
70	7,03	-	1,065531
70	7,03	-	1,065531
100	7,01	-	1,065521
100	7,05	-	1,065521
Brine	7,03	-	1,065554
Brine	7,03	-	1,065554

Table A-12: Shows concentration, pH and density of 3-cyclopentyl propionic acid in MQ-water.

3-cyclopentyl propionic acid, pH 2.			
Concentration [mM]	Measured pH	Adjusted pH	Density [g/cm ³]
1			0,997594
1			0,997594

Table A-13: Shows concentration, pH and density of 3-cyclopentyl propionic acid in MQ-water.

3-cyclopentyl propionic acid, pH 7.			
Concentration [mM]	Measured pH	Adjusted pH	Density [g/cm ³]
1	-	7,10	0,997106
1	-	7,03	0,997106
10	-	7,15	0,997379
10	-	7,14	0,997379
30	-	7,31	0,998175
30	-	7,31	0,998175
50	-	7,32	0,999028
50	-	7,32	0,999028
70	-	7,29	1,001063
70	-	7,32	1,001063
100	3,28	7,31	1,002324
100	3,28	7,31	1,002324

Table A-14: Shows concentration, pH and density of 3-cyclopentyl propionic acid in MQ-water.

3-cyclopentyl propionic acid, pH 10.			
Concentration [mM]	Measured pH	Adjusted pH	Density [g/cm ³]
1	-	11,20	0,997268
1	-	10,92	0,997268
10	-	9,95	0,997467
10	-	9,99	0,997467
30	-	10,40	0,998238
30	-	10,41	0,998238
50	-	10,65	0,999078
50	-	10,63	0,999078
70	-	10,79	0,999913
70	-	10,78	0,999913
100	3,24	10,93	1,001228
100	3,24	10,93	1,001228

Appendix B: Gibbs Adsorption Isotherm and Calculations of Surface Excess

Pyridine

Pyridine in MQ-water, pH 2:

Table B-1: The table shows the values needed for plotting the slope, surface tension vs. concentration.

Concentration [mM]	ln (c)	Surface Tension [γ]
1	0,00	72,07
10	2,30	71,90
30	3,40	71,84
50	3,91	72,12
70	4,25	72,15
100	4,61	71,93

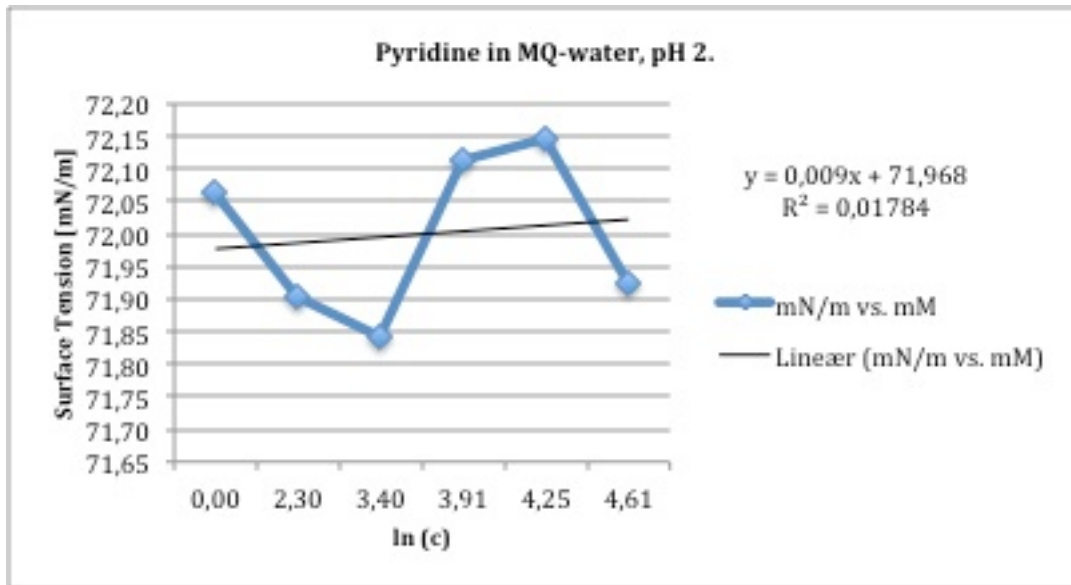


Figure B-1: The figure shows the plot of surface tension versus ln (c) and the corresponding linear relationship.

$$\Gamma = -\frac{1}{nRT} \left(\frac{d\gamma}{d\ln c} \right) \quad (B-1)$$

$$\left(\frac{d\gamma}{d\ln c} \right) = 0,009 > 0 \Rightarrow \Gamma \text{ is negative} \quad (B-2)$$

$$\Gamma = -\frac{1}{8,314 * 298} * (0,009) = -3,63 * 10^{-6} \quad (B-3)$$

Pyridine in MQ-water, pH 7:

Table B-2: The table shows the values needed for plotting the slope, surface tension vs. concentration.

Concentration [mM]	ln (c)	Surface Tension [γ]
1	0,00	71,77
10	2,30	71,34
30	3,40	70,15
50	3,91	69,09
70	4,25	68,09
100	4,61	66,66

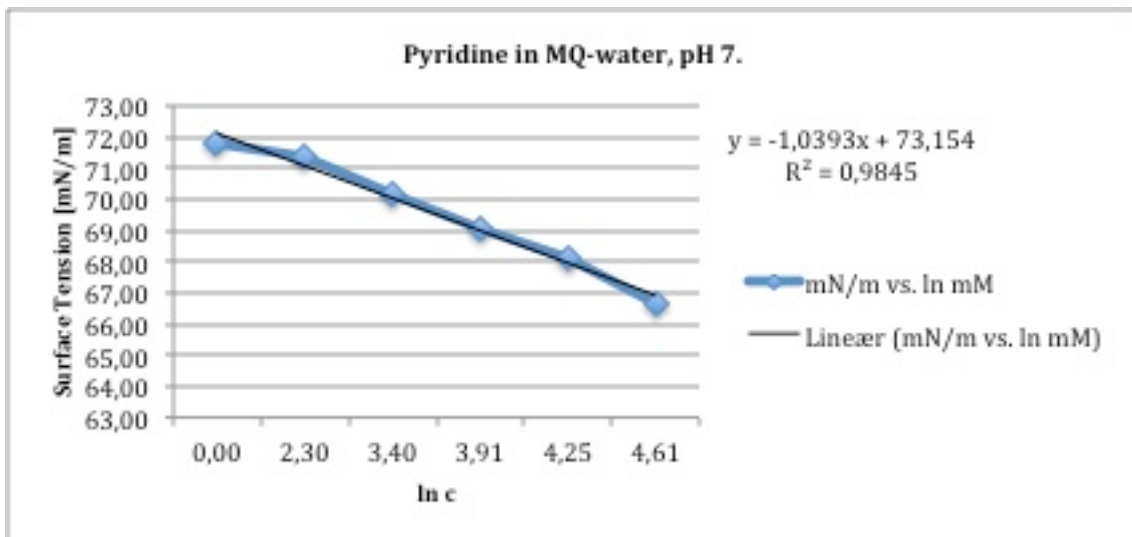


Figure B-2: The figure shows the plot of surface tension versus ln (c) and the corresponding linear relationship.

$$\Gamma = -\frac{1}{nRT} \left(\frac{d\gamma}{d \ln c} \right) \quad (\text{B-4})$$

$$\left(\frac{d\gamma}{d \ln c} \right) = -1,0393 < 0 \Rightarrow \Gamma \text{ is positive} \quad (\text{B-5})$$

$$\Gamma = -\frac{1}{8,314 * 298} * (-1,0393) = 4,2 * 10^{-4} \quad (\text{B-6})$$

Pyridine in MQ-water, pH 10:

Table B-3: The table shows the values needed for plotting the slope, surface tension vs. concentration.

Concentration [mM]	ln (c)	Surface Tension [γ]
1	0,00	71,69
10	2,30	71,13
30	3,40	70,36
50	3,91	68,86
70	4,25	68,09
100	4,61	66,80

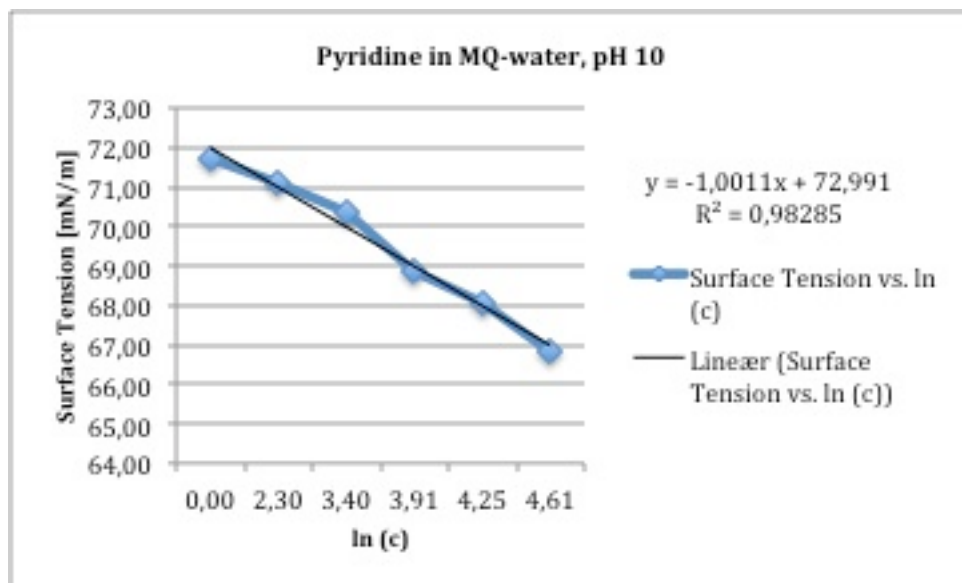


Figure B-3: The figure shows the plot of surface tension versus ln (c) and the corresponding linear relationship.

$$\Gamma = -\frac{1}{nRT} \left(\frac{d\gamma}{d \ln c} \right) \quad (\text{B-7})$$

$$\left(\frac{d\gamma}{d \ln c} \right) = -1,0011 < 0 \Rightarrow \Gamma \text{ is positive} \quad (\text{B-8})$$

$$\Gamma = -\frac{1}{8,314 * 298} * (-1,0011) = 4,04 * 10^{-4} \quad (\text{B-9})$$

Pyridine in synthetic brine, pH 2:

Table B-4: The table shows the values needed for plotting the slope, surface tension vs. concentration.

Concentration [mM]	ln (c)	Surface Tension [γ]
1	0,00	75,42
10	2,30	75,41
30	3,40	74,58
50	3,91	74,36
70	4,25	74,55
100	4,61	74,25

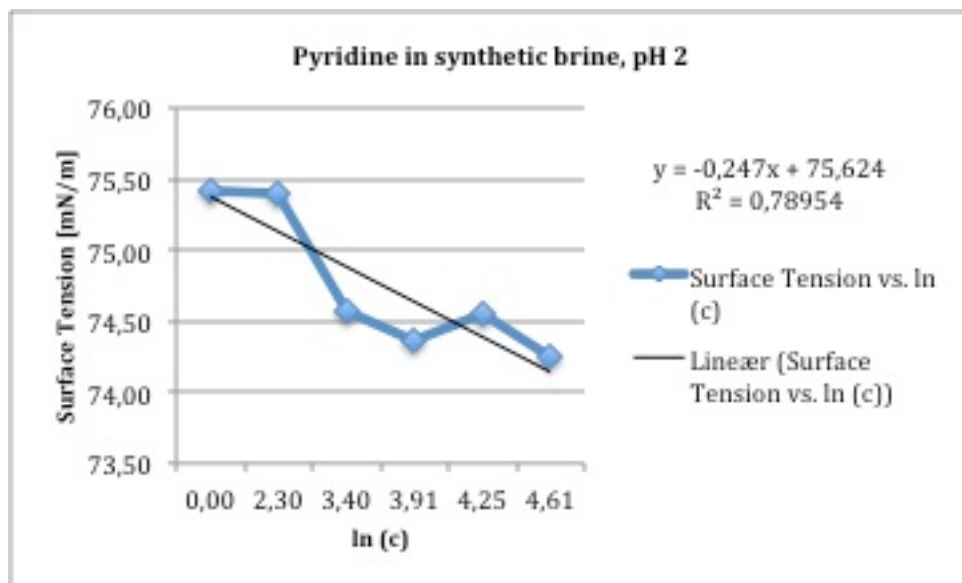


Figure B-4: The figure shows the plot of surface tension versus ln (c) and the corresponding linear relationship.

$$\Gamma = -\frac{1}{nRT} \left(\frac{d\gamma}{d \ln c} \right) \quad (\text{B-10})$$

$$\left(\frac{d\gamma}{d \ln c} \right) = -0,247 < 0 \Rightarrow \Gamma \text{ is positive} \quad (\text{B-11})$$

$$\Gamma = -\frac{1}{8,314 * 298} * (-0,247) = 9,97 * 10^{-5} \quad (\text{B-12})$$

Pyridine in synthetic brine, pH 7:

Table B-5: The table shows the values needed for plotting the slope, surface tension vs. concentration.

Concentration [mM]	ln (c)	Surface Tension [γ]
1	0,00	74,87
10	2,30	73,89
30	3,40	72,12
50	3,91	70,24
70	4,25	68,85
100	4,61	67,10

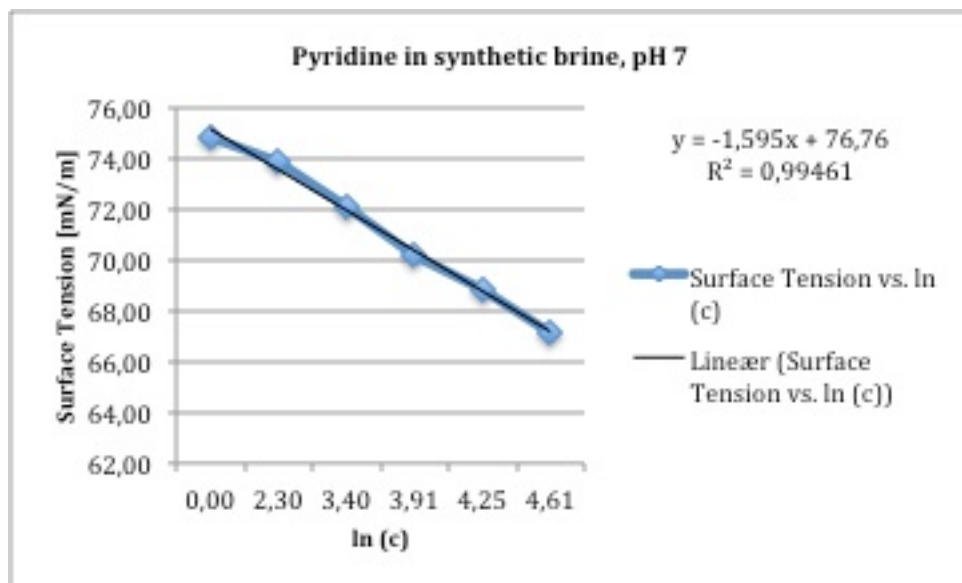


Figure B-5: The figure shows the plot of surface tension versus ln (c) and the corresponding linear relationship.

$$\Gamma = -\frac{1}{nRT} \left(\frac{d\gamma}{d \ln c} \right) \quad (\text{B-13})$$

$$\left(\frac{d\gamma}{d \ln c} \right) = -1,595 < 0 \Rightarrow \Gamma \text{ is positive} \quad (\text{B-14})$$

$$\Gamma = -\frac{1}{8,314 * 298} * (-1,595) = 6,44 * 10^{-4} \quad (\text{B-15})$$

Phenol

Phenol in MQ-water, pH 2:

Table B-6: The table shows the values needed for plotting the slope, surface tension vs. concentration.

Concentration [mM]	ln (c)	Surface Tension [γ]
1	0,00	71,66
10	2,30	70,77
30	3,40	69,25
50	3,91	67,83
70	4,25	64,57
100	4,61	62,00

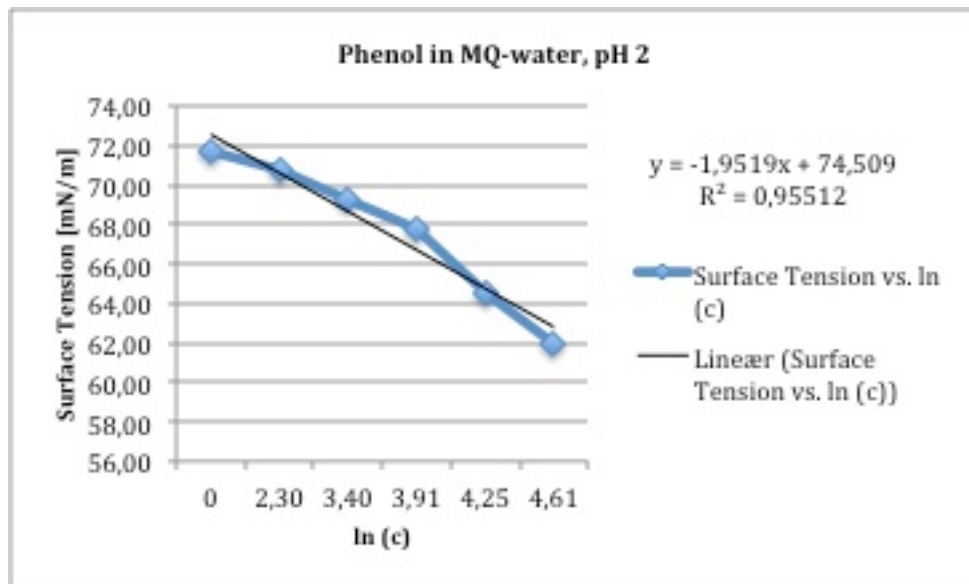


Figure B-6: The figure shows the plot of surface tension versus ln (c) and the corresponding linear relationship.

$$\Gamma = -\frac{1}{nRT} \left(\frac{d\gamma}{d \ln c} \right) \quad (\text{B-16})$$

$$\left(\frac{d\gamma}{d \ln c} \right) = -1,9519 < 0 \Rightarrow \Gamma \text{ is positive} \quad (\text{B-17})$$

$$\Gamma = -\frac{1}{8,314 * 298} * (-1,9519) = 7,88 * 10^{-4} \quad (\text{B-18})$$

Phenol in MQ-water, pH 7:

Table B-7: The table shows the values needed for plotting the slope, surface tension vs. concentration.

Concentration [mM]	ln (c)	Surface Tension [γ]
1	0,00	72,04
10	2,30	71,09
30	3,40	69,15
50	3,91	67,05
70	4,25	64,39
100	4,61	61,37

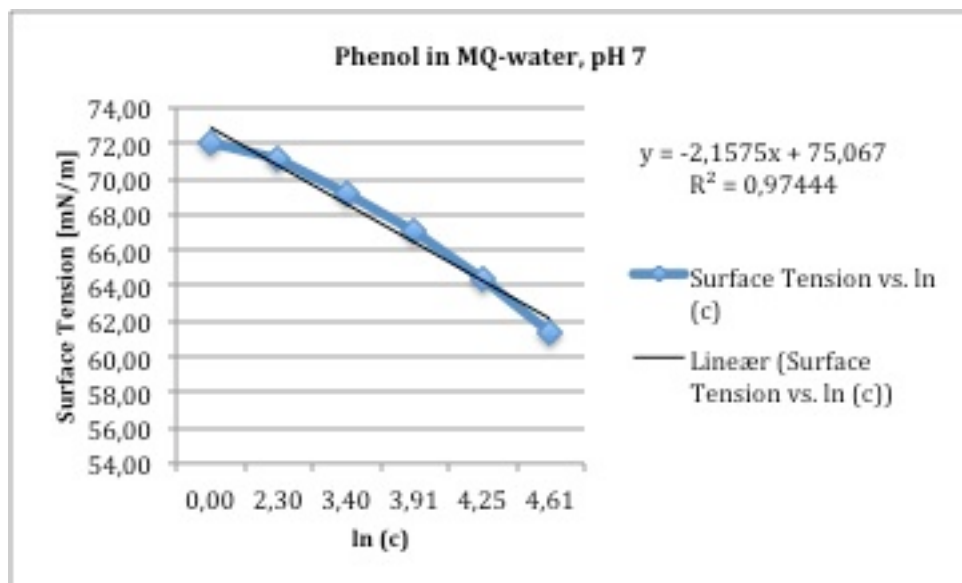


Figure B-7: The figure shows the plot of surface tension versus ln (c) and the corresponding linear relationship.

$$\Gamma = -\frac{1}{nRT} \left(\frac{d\gamma}{d \ln c} \right) \quad (\text{B-19})$$

$$\left(\frac{d\gamma}{d \ln c} \right) = -2,1575 < 0 \Rightarrow \Gamma \text{ is positive} \quad (\text{B-20})$$

$$\Gamma = -\frac{1}{8,314 * 298} * (-2,1575) = 8,71 * 10^{-4} \quad (\text{B-21})$$

Phenol in MQ-water, pH 10:

Table B-8: The table shows the values needed for plotting the slope, surface tension vs. concentration.

Concentration [mM]	ln (c)	Surface Tension [γ]
1	0,00	71,66
10	2,30	71,24
30	3,40	70,40
50	3,91	69,68
70	4,25	68,13
100	4,61	66,55

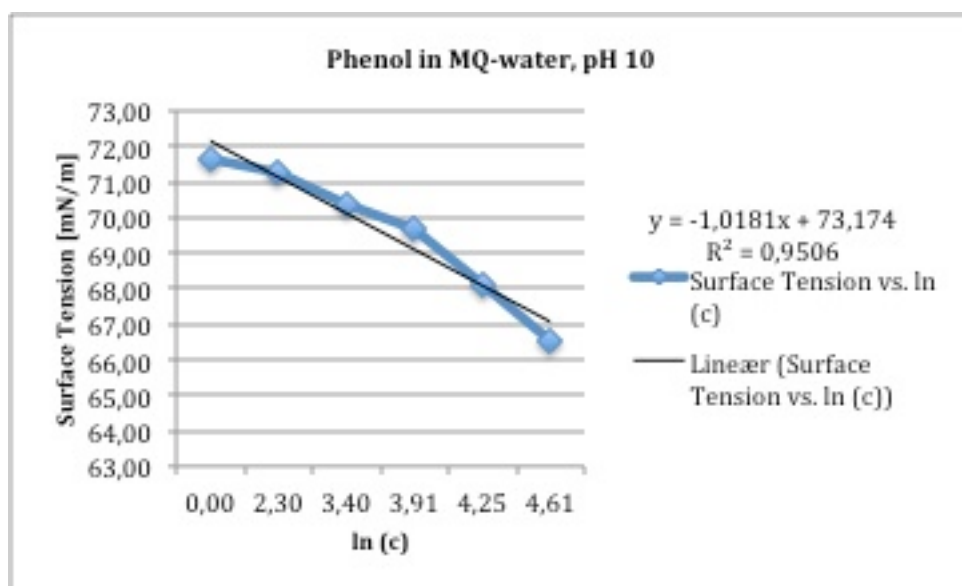


Figure B-8: The figure shows the plot of surface tension versus ln (c) and the corresponding linear relationship.

$$\Gamma = -\frac{1}{nRT} \left(\frac{d\gamma}{d \ln c} \right) \quad (\text{B-22})$$

$$\left(\frac{d\gamma}{d \ln c} \right) = -1,018 < 0 \Rightarrow \Gamma \text{ is positive} \quad (\text{B-23})$$

$$\Gamma = -\frac{1}{8,314 * 298} * (-1,018) = 4,11 * 10^{-4} \quad (\text{B-24})$$

Phenol in synthetic brine, pH 2:

Table B-9: The table shows the values needed for plotting the slope, surface tension vs. concentration.

Concentration [mM]	ln (c)	Surface Tension [γ]
1	0,00	74,90
10	2,30	74,79
30	3,40	74,43
50	3,91	73,89
70	4,25	73,46
100	4,61	72,89

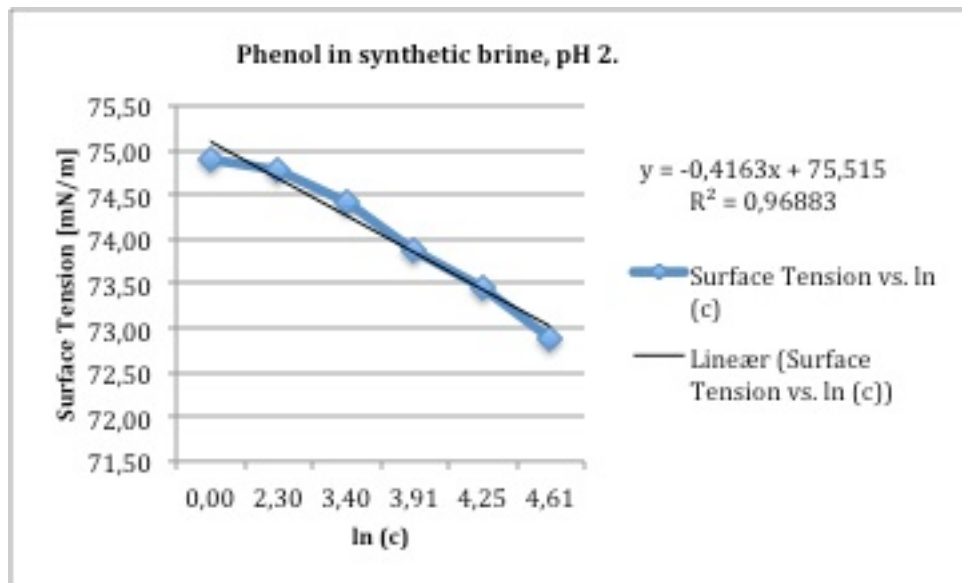


Figure B-9: The figure shows the plot of surface tension versus ln (c) and the corresponding linear relationship.

$$\Gamma = -\frac{1}{nRT} \left(\frac{d\gamma}{d \ln c} \right) \quad (\text{B-25})$$

$$\left(\frac{d\gamma}{d \ln c} \right) = -0,4163 < 0 \Rightarrow \Gamma \text{ is positive} \quad (\text{B-26})$$

$$\Gamma = -\frac{1}{8,314 * 298} * (-0,4163) = 1,68 * 10^{-4} \quad (\text{B-27})$$

Phenol in synthetic brine, pH 7:

Table B-10: The table shows the values needed for plotting the slope, surface tension vs. concentration.

Concentration [mM]	ln (c)	Surface Tension [γ]
1	0,00	74,90
10	2,30	74,79
30	3,40	74,28
50	3,91	74,39
70	4,25	73,85
100	4,61	73,05

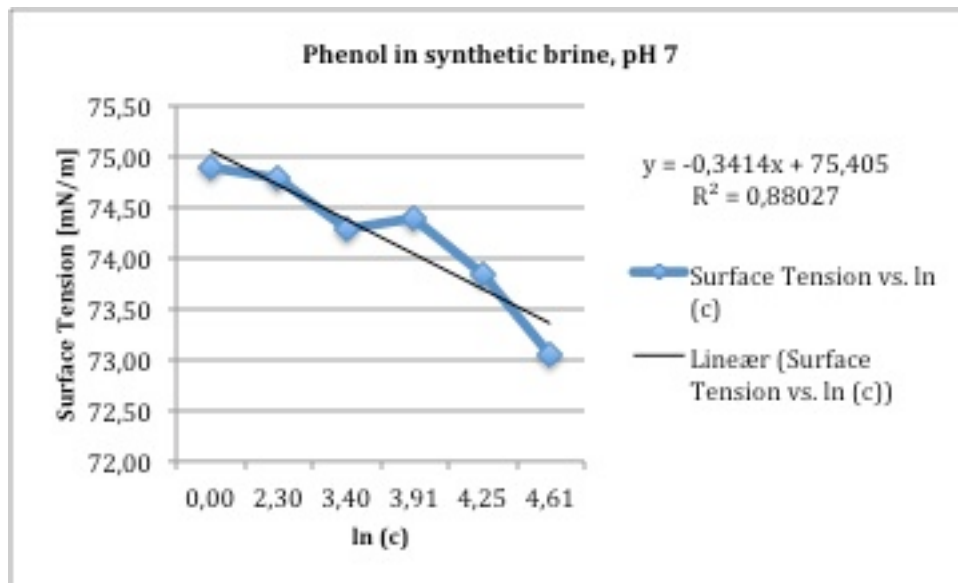


Figure B-10: The figure shows the plot of surface tension versus ln (c) and the corresponding linear relationship.

$$\Gamma = -\frac{1}{nRT} \left(\frac{d\gamma}{d \ln c} \right) \quad (\text{B-28})$$

$$\left(\frac{d\gamma}{d \ln c} \right) = -0,3414 < 0 \Rightarrow \Gamma \text{ is positive} \quad (\text{B-29})$$

$$\Gamma = -\frac{1}{8,314 * 298} * (-0,3414) = 1,38 * 10^{-4} \quad (\text{B-30})$$

3-cyclopentyl propionic acid

3-cyclopentyl propionic acid in MQ-water, pH 7:

Table B-11: The table shows the values needed for plotting the slope, surface tension vs. concentration.

Concentration [mM]	ln (c)	Surface Tension [γ]
1	0,00	71,59
10	2,30	70,92
30	3,40	70,19
50	3,91	69,57
70	4,25	67,99
100	4,61	65,84

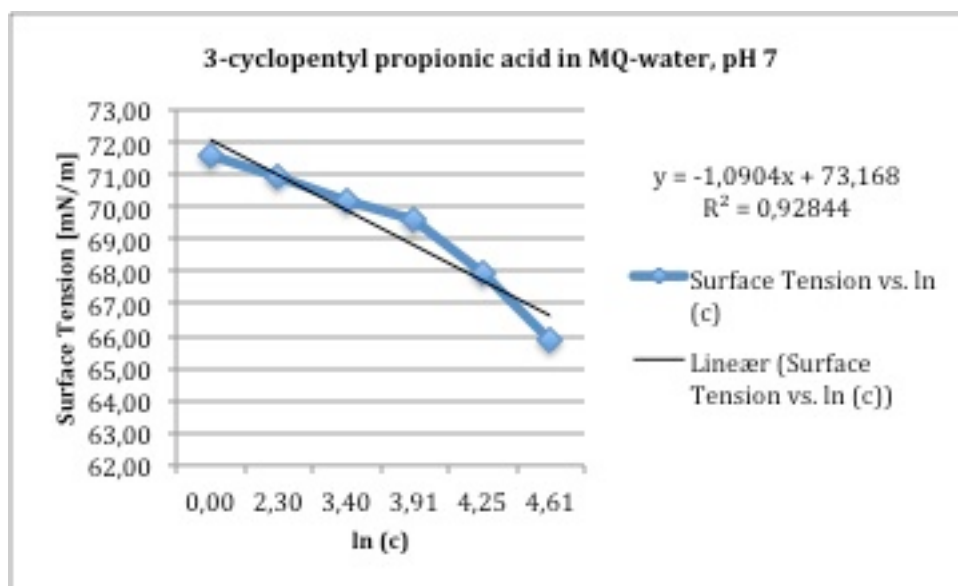


Figure B-11: The figure shows the plot of surface tension versus ln (c) and the corresponding linear relationship.

$$\Gamma = -\frac{1}{nRT} \left(\frac{d\gamma}{d \ln c} \right) \quad (\text{B-31})$$

$$\left(\frac{d\gamma}{d \ln c} \right) = -1,0904 < 0 \Rightarrow \Gamma \text{ is positive} \quad (\text{B-32})$$

$$\Gamma = -\frac{1}{8,314 * 298} * (-1,0904) = 4,40 * 10^{-4} \quad (\text{B-33})$$

3-cyclopentyl propionic acid in MQ-water, pH 10:

Table B-12: The table shows the values needed for plotting the slope, surface tension vs. concentration.

Concentration [mM]	ln (c)	Surface Tension [γ]
1	0,00	72,55
10	2,30	72,07
30	3,40	70,72
50	3,91	69,88
70	4,25	69,26
100	4,61	67,83

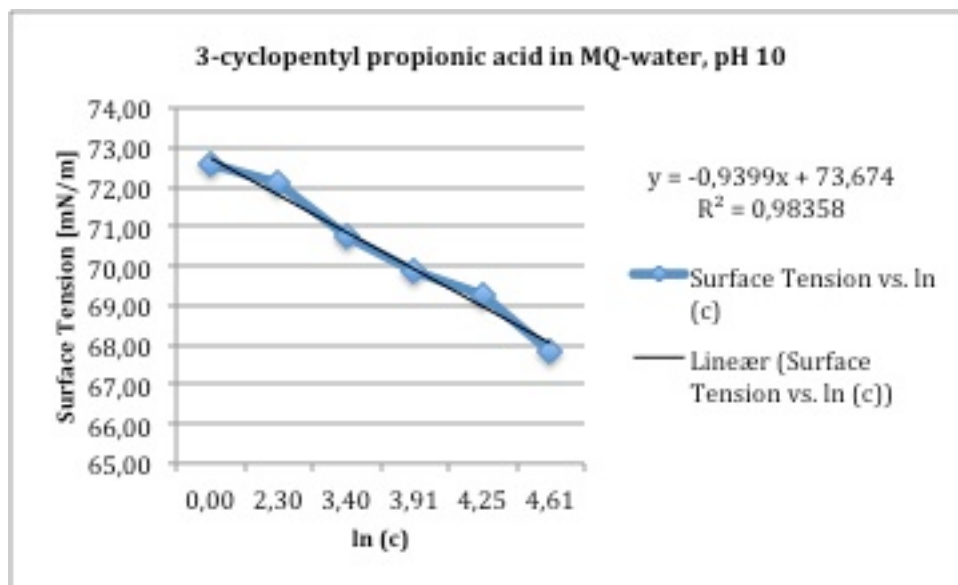


Figure B-12: The figure shows the plot of surface tension versus ln (c) and the corresponding linear relationship.

$$\Gamma = -\frac{1}{nRT} \left(\frac{d\gamma}{d \ln c} \right) \quad (\text{B-34})$$

$$\left(\frac{d\gamma}{d \ln c} \right) = -0,9399 < 0 \Rightarrow \Gamma \text{ is positive} \quad (\text{B-35})$$

$$\Gamma = -\frac{1}{8,314 * 298} * (-0,9399) = 3,79 * 10^{-4} \quad (\text{B-36})$$

Appendix C: Surface Tension vs. Surface Age

Pyridine in MQ-water

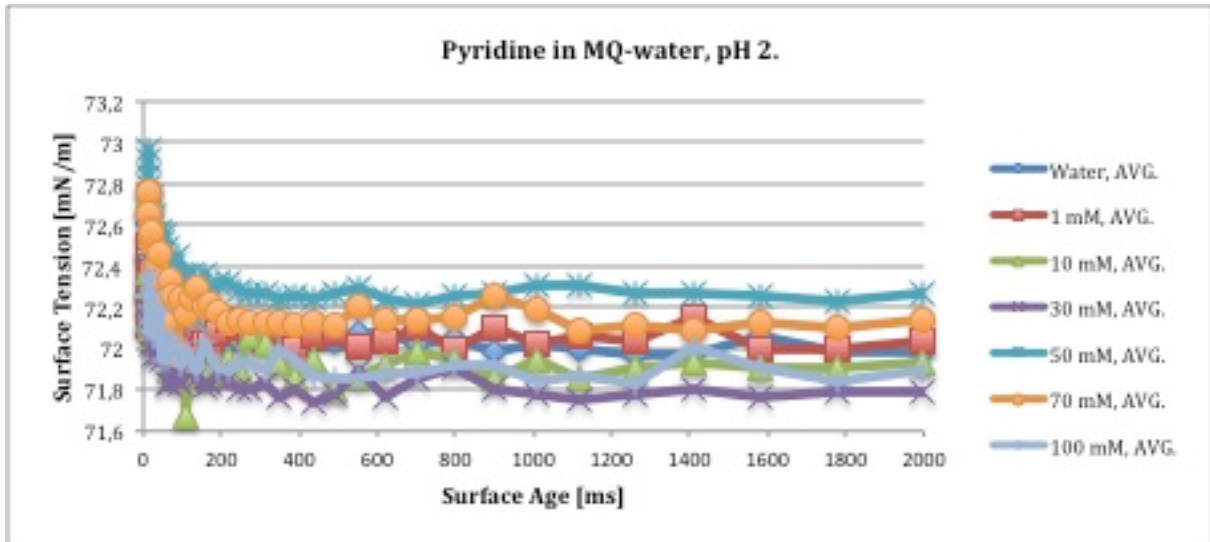


Figure C-1: Shows surface tension versus surface age for pyridine at pH 2.

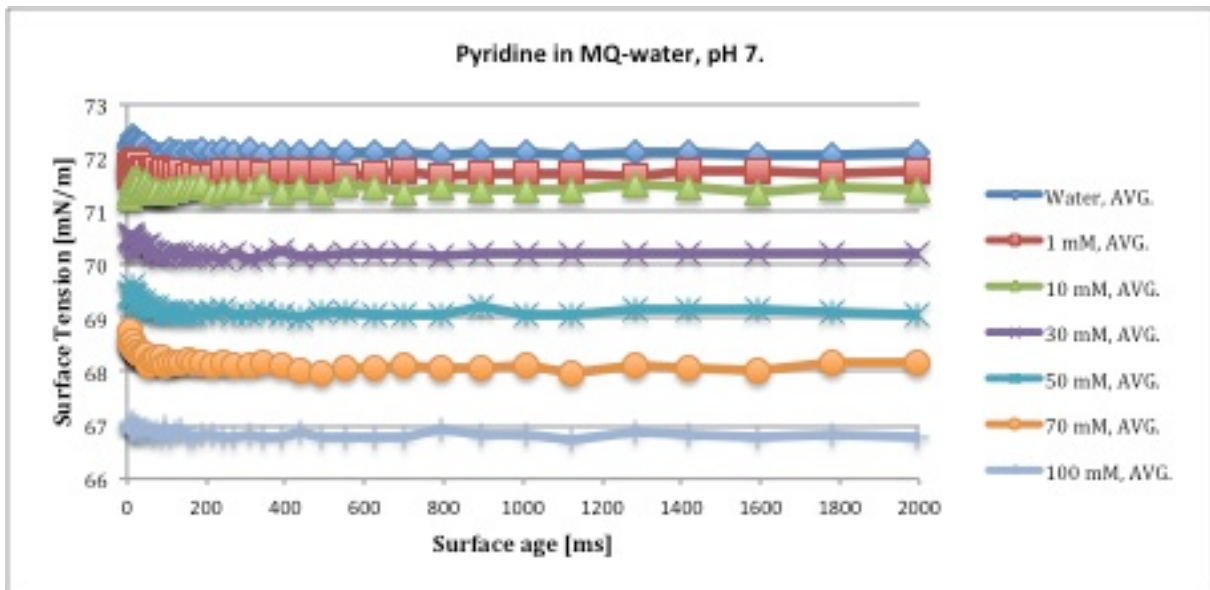


Figure C-2: Shows surface tension versus surface age for pyridine at pH 7.

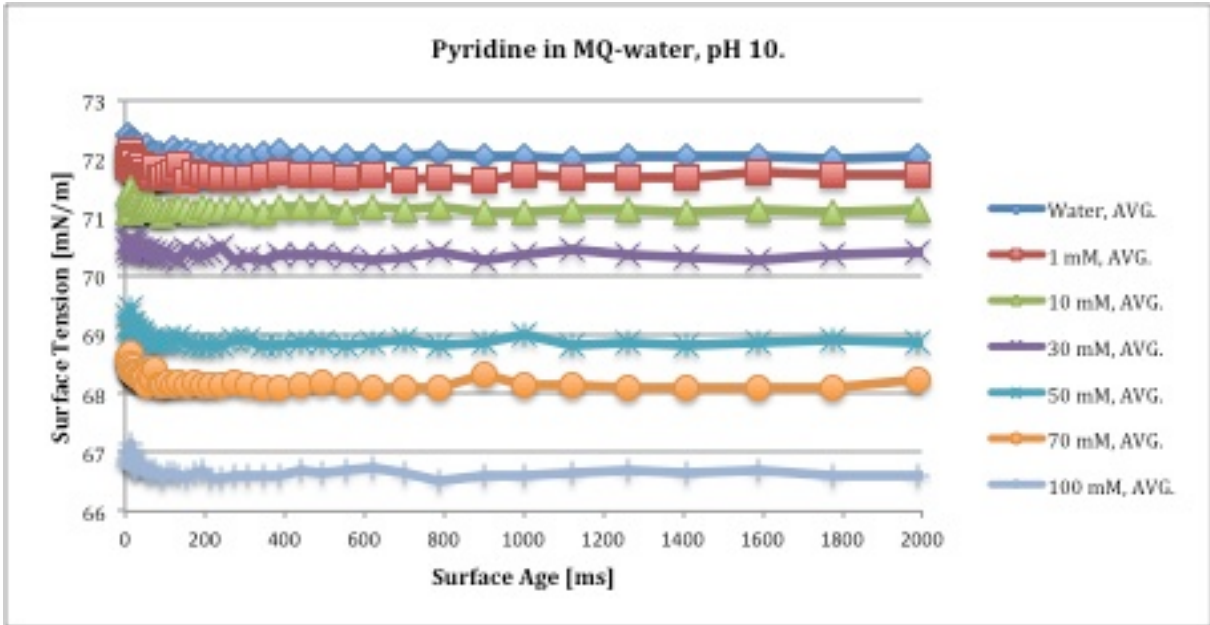


Figure C-3: Shows surface tension versus surface age for pyridine at pH 10.

Pyridine in synthetic brine

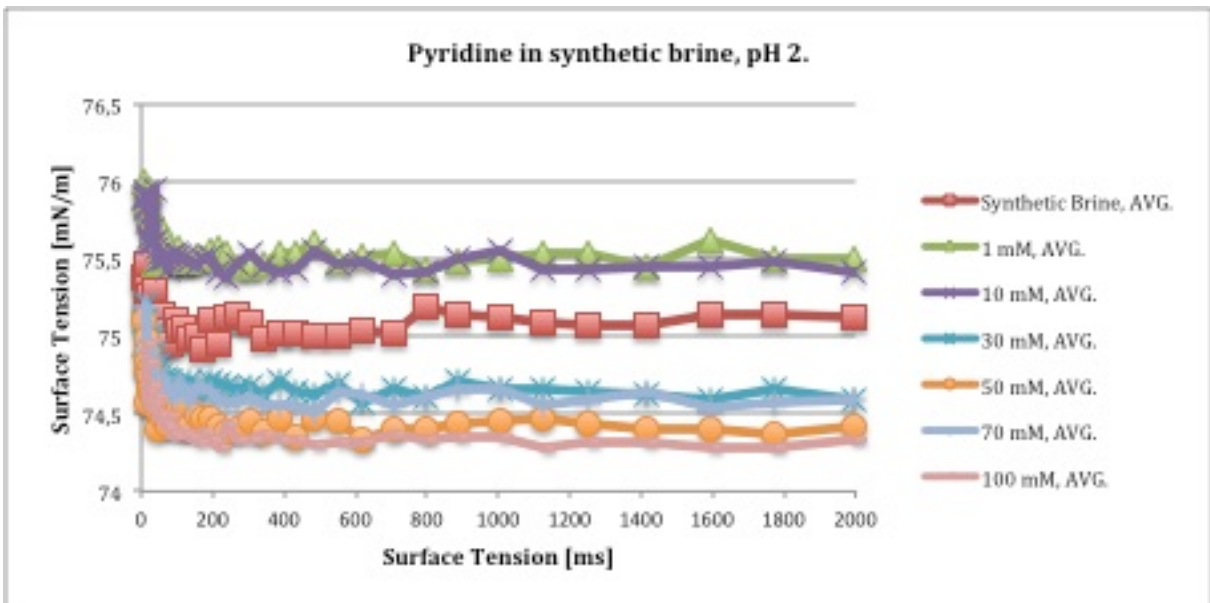


Figure C-4: Shows surface tension versus surface age for pyridine at pH 2.

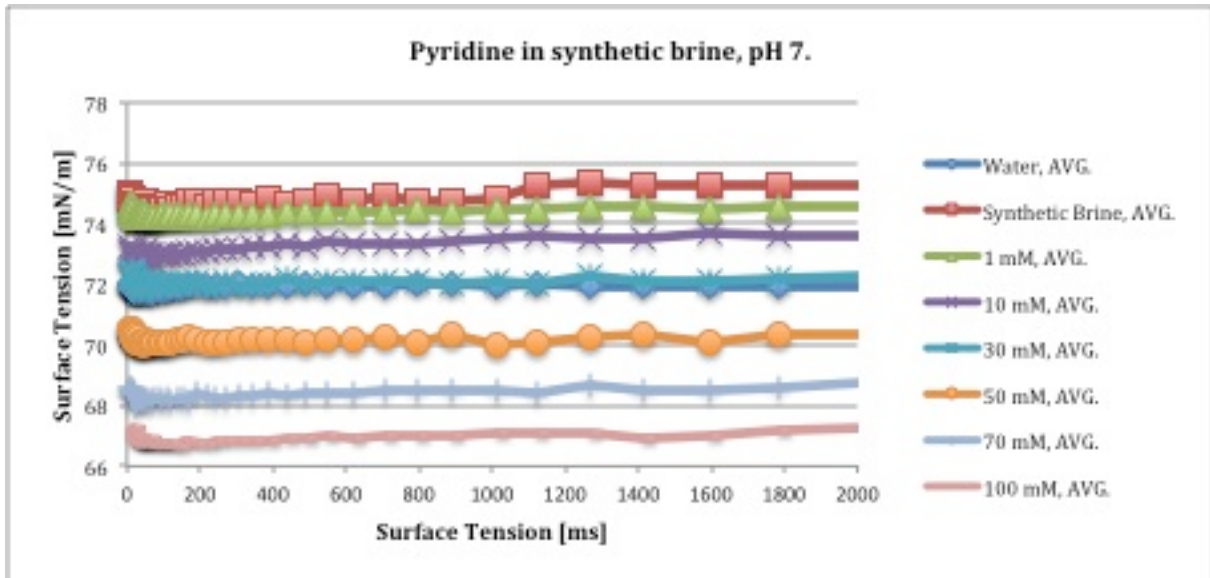


Figure C-5: Shows surface tension versus surface age for pyridine at pH 7.

Phenol in MQ-water

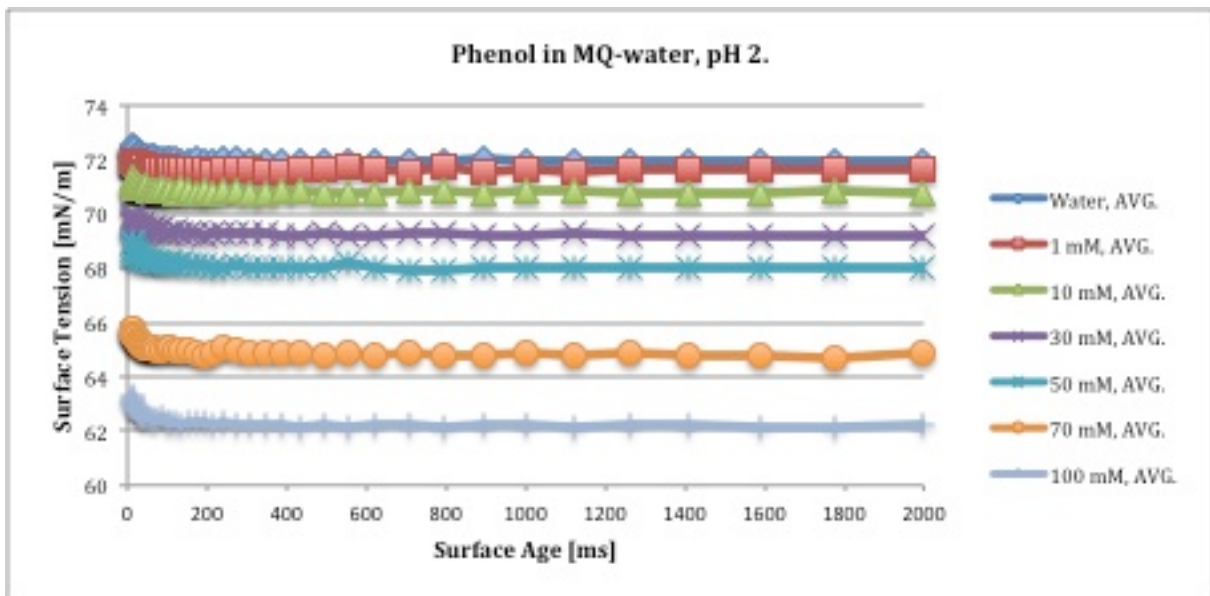


Figure C-6: Shows surface tension versus surface age for phenol at pH 2.

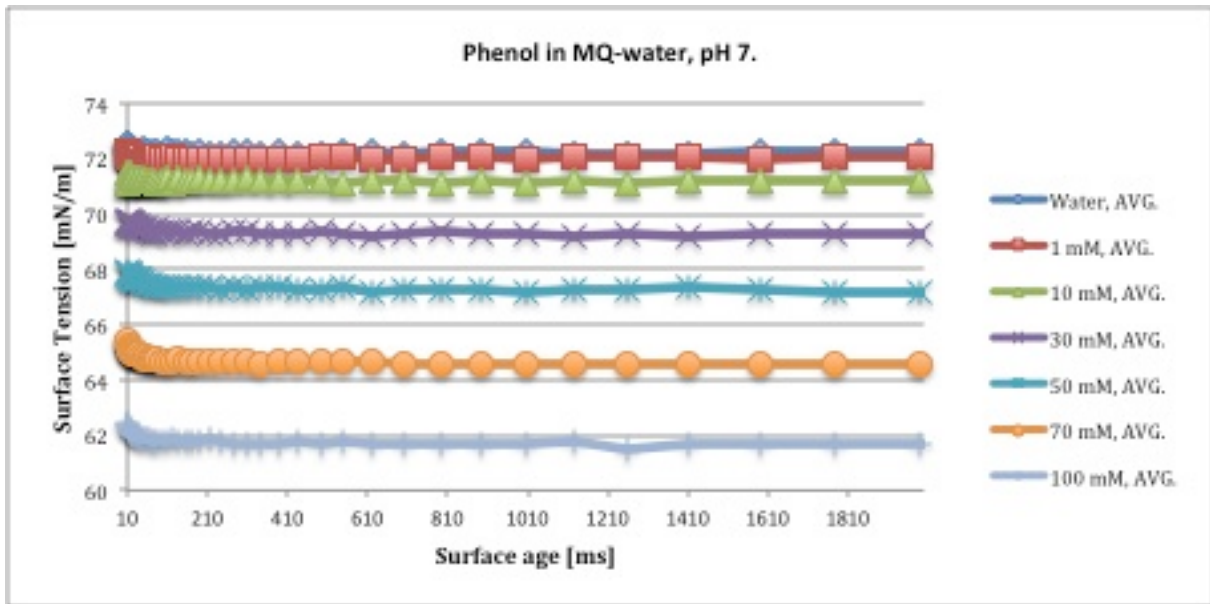


Figure C-7: Shows surface tension versus surface age for phenol at pH 7.

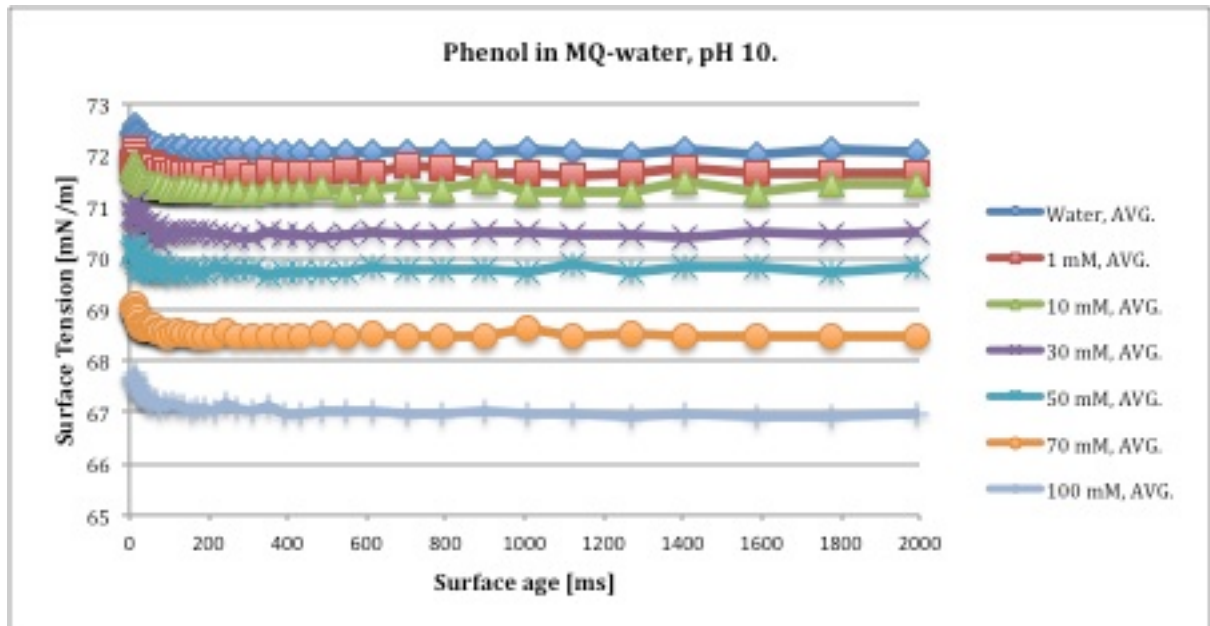


Figure C-8: Shows surface tension versus surface age for phenol at pH 10.

Phenol in synthetic brine

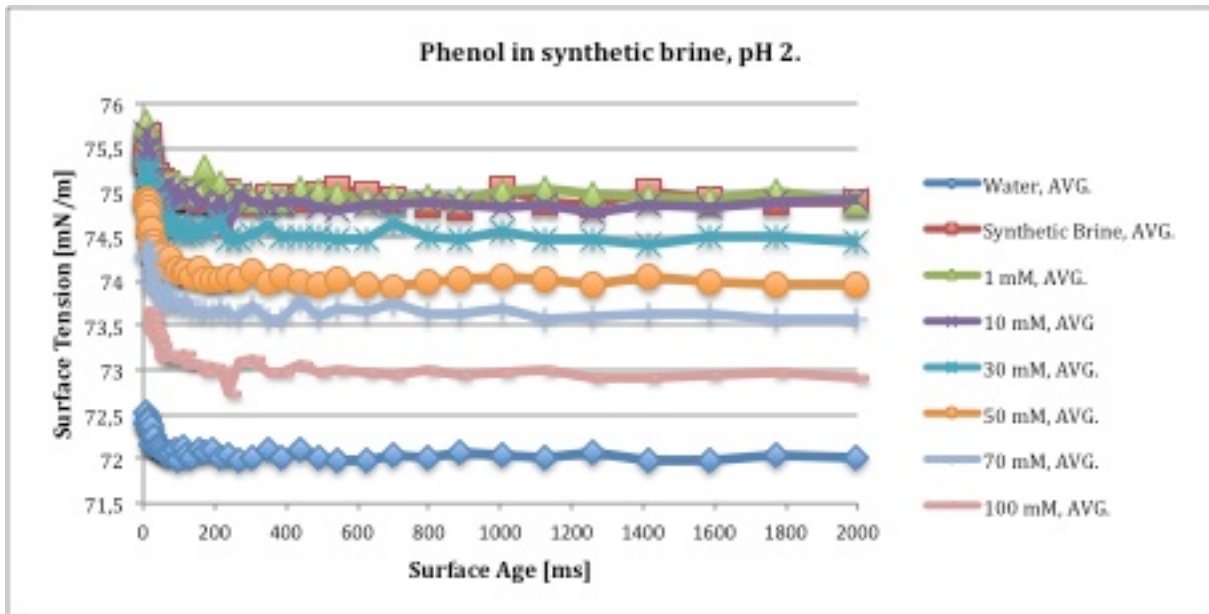


Figure C-9: Shows surface tension versus surface age for phenol at pH 2.

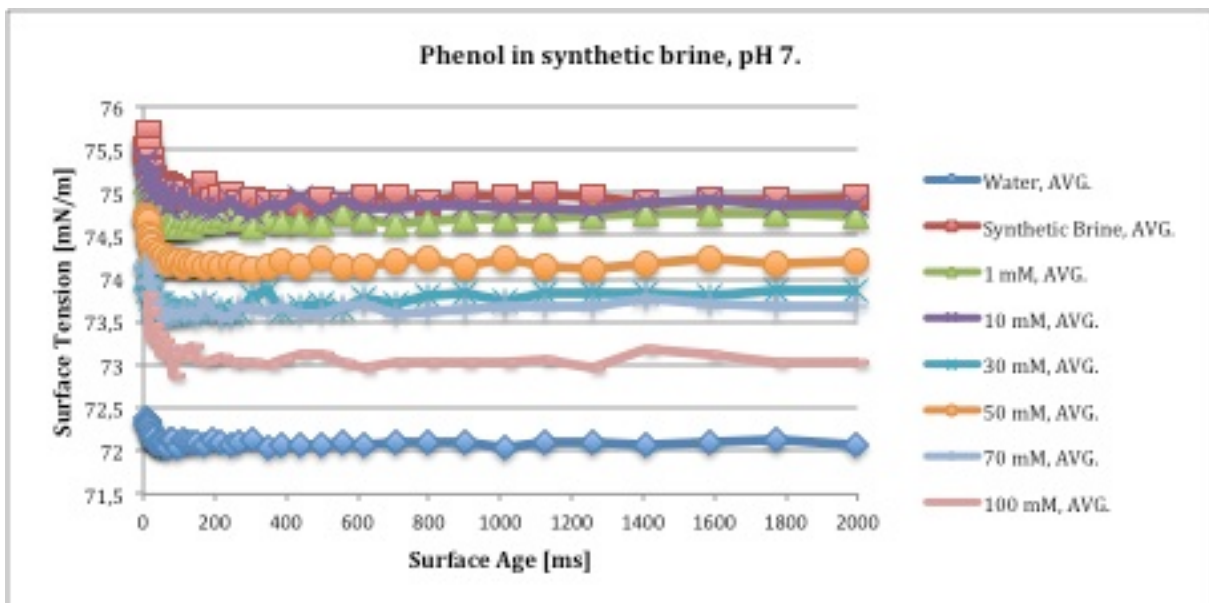


Figure C-10: Shows surface tension versus surface age for phenol at pH 7.

3-cyclopentyl propionic acid in MQ-water

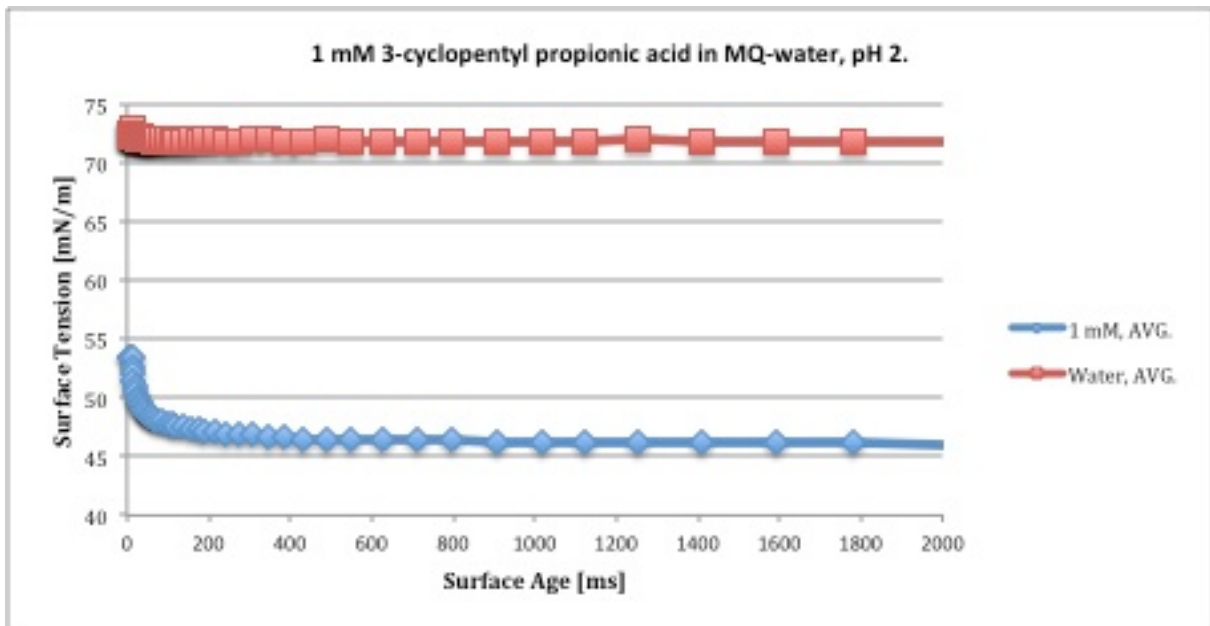


Figure C-11: Shows surface tension versus surface age for 3-cyclopentyl propionic acid pH 2.

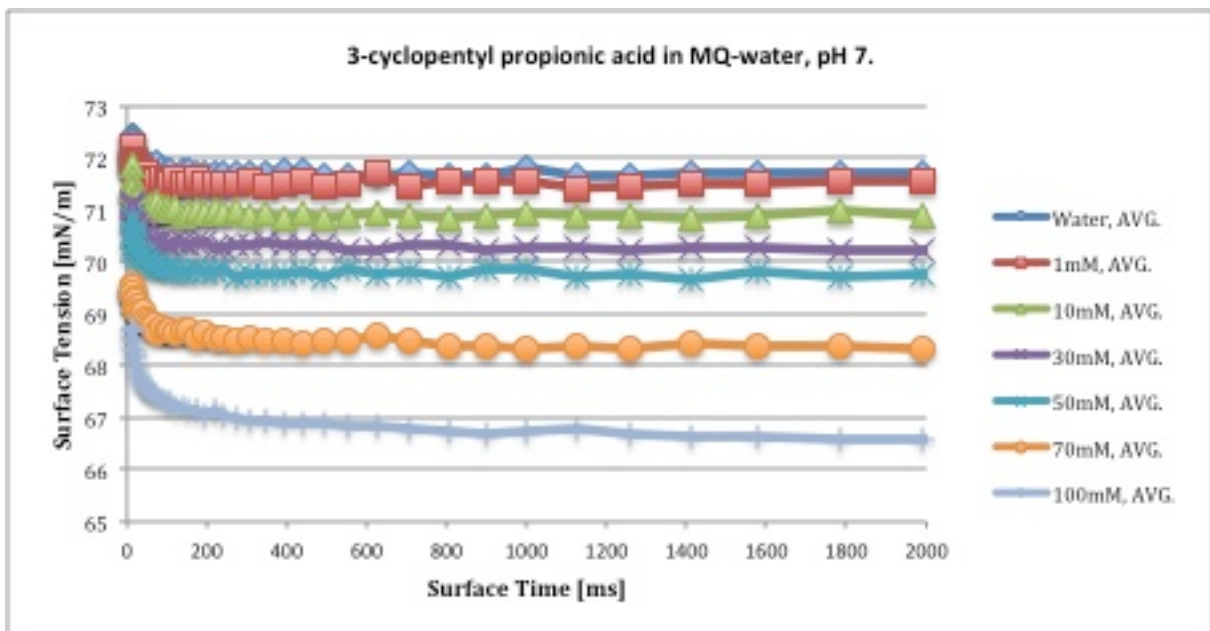


Figure C-12: Shows surface tension versus surface age for 3-cyclopentyl propionic acid pH 7.

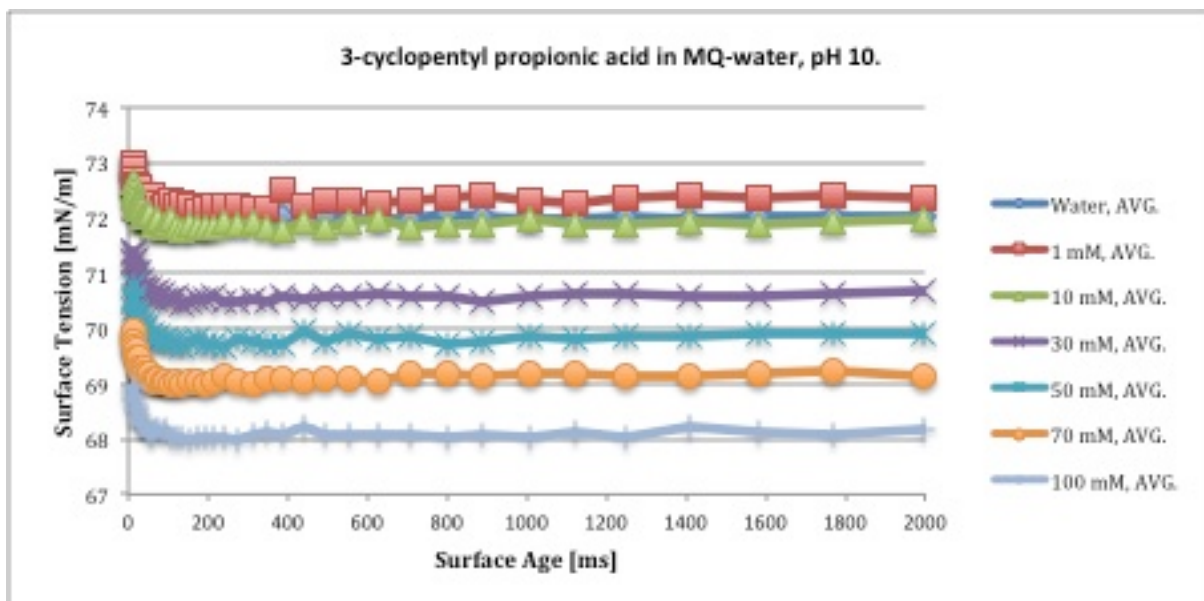




Figure C-13: Shows surface tension versus surface age for 3-cyclopentyl propionic acid pH 10.

Appendix D: Risk Assessment

NTNU	<h2>Hazardous activity identification process</h2>	Prepared by	Number	Date	
		HSE section	HMSRV2601	22.03.11	
HSE		Approved by	Page	Replaces	
		The Rector		01.12.06	

Unit: *(Department)*

Chemical Engineering

Date:

13.01.14

Line manager:

Edd Blekkan

Participants in the identification process (incl. function):
(supervisor, student, co-supervisor, others)

Gisle Øye, supervisor. Anja Johnsen, student. Mona Eftekhardadkhan, co-supervisor.

Short description of the main activity/main process:

Master project for Anja Johnsen. Interfacial characterisation of gas-liquid interfaces related to gas flotation in offshore produced water treatment

Is the project work purely theoretical? (YES/NO)

NO

*Answer "YES" implies that **supervisor is assured that no activities***

requiring risk assessment are involved in the work. If YES, briefly describe the activities below. The risk assessment form need not be filled out.



Signatures:

Responsible supervisor: _____

Student: _____

ID nr.	Activity/process	Responsible person	Existing documentation	Existing safety measures	Laws, regulations etc.	Comment
1	Making solution, Phenol.	Anja Johnsen	Safety data sheet	Gloves, lab coat, safety glasses, filter device, face shield, fume hood.	Chemical regulations	
2	Making solution, Dibenzothiophene.	Anja Johnsen	Safety data sheet	Gloves, lab coat, safety glasses, filter device, face shield, fume hood.	Chemical regulations	
3	Making solutions, Pyridine.	Anja Johnsen	Safety data sheet	Gloves, lab coat, safety glasses, filter device, face shield, fume hood.	Chemical regulations	
4	Making solutions, 3-cyclopentyl propionic acid.	Anja Johnsen	Safety data sheet	Gloves, lab coat, safety glasses, filter device, face shield, fume hood.	Chemical regulations	
5	Measuring pH	Anja Johnsen	Apparatus Card.Safety data sheet.	Gloves, lab coat, safety glasses, filter device, face shield, fume hood.	Chemical regulations	

6	Measuring the surface tension	Anja Johnsen	Apparatus Card.Safety data sheet.	Gloves, lab coat, safety glasses, fume hood.	Chemical regulations	
7	Measuring the density	Anja Johnsen	Apparatus Card.Safety data sheet.	Gloves, lab coat, safety glasses, fume hood.	Chemical regulations	
8						

	Risk assessment	HSE section	HMSRV2603	04.02.11	
		Approved by	Page	Replaces	
		The Rector		09.02.10	
HMS /KS					

Unit: *(Institute)* Chemical Engineering **Date:** 13.01.14

Line manager: Edd Blekkan

Participants in the identification process (incl. function): *(supervisor, student, co-supervisor, others)* Gisle Øye, supervisor. Anja Johnsen, student. Mona Eftekhardadkhan, co-supervisor.

Risk assessment of: Master project for Anja Johnsen. Interfacial characterisation of gas-liquid interfaces related to gas flotation in offshore produced water treatment

Signatures: *Responsible supervisor:* _____ *Student:* _____

ID nr.	Activity from the identification process form	Potential undesirable incident/strain	Likelihood:	Consequence:				Risk value (human)	Comments/status Suggested measures
			(1-5)	Human (A-E)	Environment (A-E)	Economy /material (A-E)			
1	Making solution, Phenol.	Spillage, inhalation	4	B	A	A	A	B4	Gloves, safety glasses, lab coat, face shield, filter device, fume hood.
2	Making solutions, Dibenzothiophene.	Spillage, inhalation	4	B	A	A	A	B4	Gloves, safety glasses, lab coat, face shield, filter device, fume hood.
3	Making solutions, Pyridine.	Spillage, flammable, inhalation	4	B	A	A	A	B4	Gloves, safety glasses, face shield, filter device, lab coat, fume hood.
4	Making solutions, 3-cyclopentyl propionic acid.	Spillage, flammable inhalation	3	B	A	A	A	B3	Gloves, safety glasses, lab coat, face shield, filter device, fume hood.
5	Measuring the surface tension	Capillary may break.	1	A	A	B	A	A1	Gloves, safety glasses, lab coat, fume hood. Have to handle the capillary with care.
6	Measuring the density	Spillage	1	A	A	A	A	A1	Gloves, safety glasses, lab coat, fume hood.

7	Measuring pH	Spillage	1	A	A	A	A	A1	Gloves, safety glasses, face shield, filter device, lab coat, fume hood.
---	--------------	----------	---	---	---	---	---	----	--

Risk value = Likelihood (1, 2 ...) x consequence (A, B ...). Risk value A1 means very low risk. Risk value E5 means very large and serious risk

Likelihood		Consequence					
Value	Criteria	Grading		Human	Environment	Economy/material	
1	Minimal: Once every 50 year or less	E	Very critical	May produce fatality/ies	Very prolonged, non-reversible damage	Shutdown of work >1 year.	
2	Low: Once every 10 years or less	D	Critical	Permanent injury, may produce serious health damage/sickness	Prolonged damage. Long recovery time.	Shutdown of work 0.5-1 year.	
3	Medium: Once a year or less	C	Dangerous	Serious personal injury	Minor damage. Long recovery time	Shutdown of work < 1 month	
4	High: Once a month or less	B	Relatively safe	Injury that requires medical treatment	Minor damage. Short recovery time	Shutdown of work < 1week	
5	Very high: Once a week	A	Safe	Injury that requires first aid	Insignificant damage. Short recovery time	Shutdown of work < 1day	

MATRIX FOR RISK ASSESSMENT

CONSEQUENCE	Very critical	E1	E2	E3	E4	E5
	Critical	D1	D2	D3	D4	D5
	Dangerous	C1	C2	C3	C4	C5
	Relatively safe	B1	B2	B3	B4	B5

	Safe	A1	A2	A3	A4	A5
		Minimal	Low	Medium	High	Very high
		LIKELIHOOD				

Explanation of the colors used in the risk matrix.

Color	Description
Red	Unacceptable risk. Safety measures must be implemented.
Yellow	Measures to reduce risk shall be considered.
Green	Acceptabel risk.